Energy & Buildings 324 (2024) 114921

Contents lists available at ScienceDirect

Energy & Buildings

journal homepage: www.elsevier.com/locate/enb

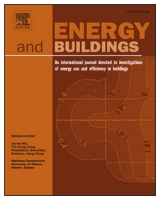

Investigation on the overall performance of hydrogel-based thermochromic windows with various structures

Chuyao Wang , Sai Liu , Xin Li , Qiuyi Shi , Wenqi Wang , Yang Fu , Jianheng Chen , Chi Yan Tso *

School of Energy and Environment, City University of Hong Kong, Hong Kong, PR China

ARTICLE INFO

Keywords:
Thermochromism
Window structures
Building energy saving
Thermal comfort
Daylighting performance

ABSTRACT

Thermochromic (TC) windows have attracted extensive attention due to their potential for improving building performance through the variation of optical properties in response to temperature. However, past studies on TC windows at the building scale primarily focused on optimizing and evaluating the properties of TC materials, with little attention paid to the varying window structures frequently encountered in engineering applications. In this study, the building performance of hydrogel-based TC windows was investigated from the structural perspective. A comprehensive simulation framework was developed, integrating overall performance simulations of energy consumption and indoor comfort. Using a self-fabricated hydrogel TC glass and an office building as the case study, the impact of the optical properties of the substrate glass on single, double, vacuum, and ventilation TC windows was analyzed. The results indicated that the optimal extinction coefficients for the studied windows range from 55 to 105 m^{-1} for visible irradiation and from 155 to 255 m^{-1} for near-infrared irradiation. Subsequently, the overall performance improvements of these types of TC windows relative to corresponding static versions were calculated. It was found that the impacts of TC glass on these four windows varied significantly. The electricity usage was reduced by 33 ~ 53 %, and the thermal comfort and visual comfort were enhanced by –22 ~ 20 % and 72 ~ 100 %, respectively. This study reveals in detail how the TC window structure affects various aspects of building performance, aiming to inspire and guide the consideration of window structure in the practical applications of TC glass.

1. Introduction

With the development of modern cities, glazed facades are becoming increasingly prevalent in the outer skins of high-rise buildings to meet aesthetic, daylighting, and visual requirements [1]. However, their poor thermal insulation and the transmission of solar irradiation significantly increase building energy consumption. Statistics indicate that glazed facades account for approximately 37 % of the total solar heat gain and 40 % of the total heat loss of building envelopes [2]. To address these energy challenges, several innovative technologies have been explored, with smart windows emerging as a particularly promising solution attracting significant research interest [3]. Smart windows can adaptively regulate the optical properties of glazed facades in response to environmental stimuli. The potential impact is substantial, with an estimation suggesting that completely replacing the existing window stock with smart windows could save over 1.3×10^{15} kJ/year in building energy [4]. Among the various smart window technologies, thermochromic (TC) windows stand out as a highly promising candidate due to their low cost, simple configuration, and zero energy input [5]. They can dynamically adjust their transmittance with temperature changes, thereby enhancing building energy efficiency. Since Granqvist et al. [6] first proposed VO_2-based smart windows in 1987, TC smart windows have been widely studied, from materials science to building applications.

1.1. Literature review

Among the TC materials currently under extensive investigation, VO_2, perovskite, and hydrogels stand out as prominent candidates. At the material scale, research primarily focuses on improving key performance metrics of TC glass, such as transition temperature, optical properties, and stability [7]. For instance, the transition temperature of VO_2 is commonly manipulated from its original 68 °C to near room temperature through element doping such as W [8], Mg [9], Ta [10], or multi-element co-doping [11,12]. The transition temperature of hydrogel can be fine-tuned by incorporating polymers like polyacrylamide for decreasing [13] and dimethylacrylamide for increasing [14]. For

* Corresponding author.
E-mail address: chiytso@cityu.edu.hk (C. Yan Tso).

https://doi.org/10.1016/j.enbuild.2024.114921
Received 30 July 2024; Received in revised form 3 October 2024; Accepted 14 October 2024
Available online 18 October 2024
0378-7788/© 2024 Elsevier B.V. All rights are reserved, including those for text and data mining, AI training, and similar technologies.

Nomenclature

Abbreviation

CDF	Cumulative distribution function
DGP	Discomfort glare probability
IGDB	International glass database
PDF	Probability density function
PMV	Predicted mean vote
PPD	Predicted percentage of dissatisfied
TC	Thermochromic
UDI	Useful daylight illuminance

Symbol

T	overall glazing transmittance
R	overall glazing reflectance
τ	transmissivity in glass interior
r	reflectivity on glass interface
λ	wavelength (um)
φ	AM1.5 solar spectrum ($W \bullet m^{-2} \bullet um^{-1}$)
ϕ	CIE photopic luminous efficiency

Superscript

c	cold state
h	hot state
$beam$	beam irradiation
dif	diffuse irradiation
f	front side
b	back side

Subscript

g	substrate glass
i,j	sub glass between interface i and j

perovskite TC material, the transition temperature can be modulated by ambient humidity [15] or additives [16]. To enhance the optical properties of TC materials, strategies such as material blending and microstructure design are often employed [7]. Guo et al. [17] developed the hydrogel embedded with carrageenan and Na_2SiO_3, resulting in the visible transmittance of 87.37 % and the solar modulation ability of 69.65 %. Zhang et al. [18] fabricated the $V_{0.8}W_{0.2}O_2$@SiO_2-doped TC microgel, showcasing a visible transparency of 92.48 % and a solar modulation ability of 77.20 %. In the realm of microstructure design, the utilization of multilayer-film and core–shell structures stands as a prevalent method [19]. Jin et al. [20] introduced the VO_2 multilayer films incorporating ZnO as a buffer and anti-reflective layer, resulting in an enhancement of solar modulation ability by 14 % and luminous transmittance by 50 %. Researchers such as Wu et al. [21], Wang et al. [22], and Zhao et al. [23] employed materials like CaF_2, SiO_2, and polymers to encapsulate VO_2 particles, forming core–shell structures to enhance visible transmittance or solar modulation ability. In efforts to improve the stability of TC materials, Liu et al. [24] demonstrated a significant reduction in decay rates by 37 times through the application of a superhydrophobic coating on perovskite TC materials. Likewise, Liang et al. [25] augmented the UV and moisture resistance of VO_2 TC glass by coating it with TiO_2 and SiO_2 films, resulting in a remarkable lifespan of 1777 days. Jiang et al. [26] pioneered a hydrogel system with polyethylene glycol, leveraging its antifreeze and regenerative properties to bolster stability. Researchers are increasingly focusing on addressing the issues of high hysteresis width and long response times in TC materials. For instance, Zhu et al. [27] innovated a solid–liquid hydrogel, achieving complete transitions within 5 s. Liu et al. [28] replaced the I element in $MAPbI_3$ perovskite TC material with the Cl, achieving a narrower transition hysteresis width.

Different from the material scale, research at the building scale emphasizes building performance, including energy consumption, indoor daylighting, and thermal environments. Researchers often evaluate the building performance based on the hypothetical properties or theoretical value of TC glass to understand how tuning material properties impacts overall building performance. Regarding transition temperature, Araújo et al. [29] determined the optimal transition temperatures through simulation and the optimized solution could achieve a 15 % energy reduction. Tao et al. [30] simulated the detailed thermal behavior of TC glass considering the inhomogeneous transition of TC material, finding the best transition temperature at 25–35 °C. In terms of the switching delay of TC glass, Arnesano et al. [31] compared different transition profiles of TC glazing to determine an optimal configuration. Khaled et al. [32] developed a heat transfer model to evaluate the impact of switching delay, finding that longer switching times worsened energy performance. Regarding optical properties, Wu et al. [33] investigated the effect of spectrally selective modulation in TC glass on building performance. Liang et al. [34] conducted a comprehensive analysis to investigate the separate effects of near-infrared and visible modulation of TC glass. Additionally, there are studies on optimizing building performance from the perspective of microstructure. For instance, Hu et al. [35] theoretically investigated the structure of VO_2 based on a Fabry-Perot resonant cavity, achieving radiative cooling in hot states while modulating near-infrared radiation. Haratoka et al. [36] examined the microscale impact of VO_2 particle diameter and concentration on building performance, identifying optimal VO_2 particle configurations for various regions. Zhao et al. [37] optimized the thickness of multilayer VO_2 TC films by considering film interference, using building performance as the optimization objective. Haratoka et al. [38] optimized the particle concentration and coating thickness of VO_2 films via the transfer matrix method, revealing up to 26 % and 9 % energy savings potential in relatively hot and cold climates, respectively.

To analyze the building performance of TC windows more precisely, experimental and simulation research using real TC glass is becoming increasingly popular. These studies offer more convincing results, better reflecting the actual characteristics of TC windows. Mohammad et al. [39] fabricated a TiO_2@W-VO_2 TC glazing with increased transmittance and investigated its daylighting performance in a room setting. Aburas et al. [40] created the VO_2 films of varying thicknesses and delved into the intricate relationship between daylighting and building energy saving. He et al. [41] assessed the energy-saving performance of a fabricated hydrogel TC glass by integrating indoor set-point correction based on thermal comfort. In addition to performance evaluation, some advancements have been made to improve TC glass functionality. Sun et al. [42] introduced a hydrogel TC glass integrated with parallel slat transparent insulation materials. Subsequent work by Ming et al. [43] demonstrated that this system could reduce summer heat gain by 30 % while reducing winter heat loss by 20 %. Wang et al. [44] and Ding et al. [45] proposed the hydrogel TC window featuring opposite reflectivity on the front and back sides, enabling tunability of mid-infrared radiation through manual reversal. In addition, Liu et al. [46] and Xu et al. [47] combined hydrogel TC glass with PV cells, using the high reflectivity of hydrogel in hot state to increase the PV power. Currently, the direct application of TC glass in actual buildings and the evaluation of overall performance are also emerging. Teixeira et al. [48] conducted the performance evaluation of TC glazing installed in commercial buildings, using a numerical model calibrated by experimental data. Es-sakali et al. [49] and Shi et al. [50] built the experimental platforms to test TC glass, demonstrating improvements in energy consumption and indoor visual-thermal comfort. Liang et al. [51] conducted experimental tests to assess the influence of different thermochromic tint states on human responses. Subsequently, Shen et al. [52] compared different types of TC glazing in

terms of building performance, taking the dynamic solar spectrum into account.

1.2. Research gap and motivation

The above literature review indicates that the improvement of material metrics and the optimization or evaluation of building performance constitute the overall research framework for TC windows. Numerous studies at the building scale have also demonstrated that TC windows hold significant potential for positively regulating building energy consumption and indoor environment. The driving mechanism behind these benefits lies in the ability of TC materials to alter their optical properties in response to temperature changes. In practical applications, the window structures, including the window types and the substrate glass, play a crucial role in influencing the thermal dynamics of the TC material, thereby affecting the ability of TC material to regulate building performance. This influence can be further elucidated as follows:

(1) Current buildings feature a variety of window types, mainly including single, double, vacuum, and ventilation glazing, each with distinct thermal behaviors. For instance, Michaux et al. [53] indicated that the glass temperature in ventilation glazing is 5 ~ 8 °C lower than in double glazing. Huang et al. [54] observed that the outer surface temperature of vacuum glazing is around 4 °C higher than that of double glazing. When TC glass is integrated into different window types, these differences in glass temperature will result in markedly different effects on building performance. Therefore, careful consideration of window type is essential when applying TC glass in buildings.

(2) TC glass typically consists of the TC material coated on the substrate glass, the critical component of the TC window. The optical properties of the substrate glass directly alter the transition state of the TC material. In certain instances, using substrate glass with high solar absorption can enhance building performance by accelerating the transition of the TC material state. Liu et al. [55] applied TC materials to substrate glass with near-infrared absorption to extend the time that TC material remains in the hot state. However, the glass with excessively high absorbance may cause poor daylighting performance [56]. Thus, the selection of substrate glass must be carefully optimized to achieve both energy efficiency and indoor environmental quality.

From the discussion above, it is evident that the window structure has a significant influence on the performance of TC glass in practical applications. However, past building-scale studies have largely neglected this critical factor, thus leading to a significant research gap. First, most previous studies have typically concentrated on one window type, usually single or double pane, which has created a gap in understanding how the same TC glass performs across different window types. This understanding is essential for optimizing TC glass applications in diverse building contexts. Therefore, a quantitative investigation is necessary to accurately assess the improvements in building performance when TC glass is integrated into various window types. Secondly, past research on TC windows has predominantly focused on the overall optical properties of TC glass, encompassing both the substrate glass and TC materials. This focus has led to limited quantitative analyses regarding how the substrate glass itself affects building energy efficiency and indoor environmental quality. Addressing these gaps is crucial for developing a more comprehensive understanding of TC glass's role in enhancing building performance.

Motivated by the research gaps identified above, this study conducts a comprehensive analysis of the performance of TC windows from the structural perspective. Taking hydrogel-based TC glass as an example, a comprehensive evaluation framework is developed to analyze the overall building performance of different types of TC windows and to optimize the optical properties of substrate glass. The detailed workflow of this article is as follows: First, the studied window types and optimized optical parameters of the substrate glass are introduced. Then, the hydrogel glass is fabricated and characterized, and the simulation methodology for evaluating the overall building performance of different window structures is described. Subsequently, the impact of the optical properties of the substrate glass on building performance is analyzed and optimized. Based on the optimized optical parameters, different types of TC windows are compared. Finally, the conclusions and suggestions for the application of TC glass based on this study are provided to promote the future practical application of TC glass. This research addresses a crucial but underexplored aspect of TC glass application, aiming to offer a comprehensive understanding of how the TC window structures influence building dynamics.

2. Description of window structures and optimization parameters

Hydrogels have garnered extensive attention in the field of TC windows due to their high stability and transition temperatures close to room temperature [57]. They consist of the three-dimensional cross-linked networks composed of water and hydrophilic polymer chains [7]. The working principle of hydrogel-based thermochromic windows is shown in Fig. 1. The hydrogel is encapsulated between two sheets of substrate glass in a sandwich structure. At temperatures below the transition temperature, the polymer chains in the hydrogel exhibit hydrophilic properties due to the intermolecular hydrogen bonds between them and the surrounding water molecules. This results in the hydrogel being transparent, as the orderly arrangement of polymer chains and water allows light to pass through with minimal scattering, giving the hydrogel optical properties similar to those of water. When the temperature rises above the transition temperature, the hydrogen bonds between the polymer chains and water molecules break. This causes the polymer chains to lose their hydrophilic nature and become hydrophobic, leading to a collapse and aggregation of the polymer network. This phase transition causes the hydrogel to become opaque or translucent, as the aggregated polymer chains scatter incident light, reducing the transmission of light through the hydrogel.

As described in Section 1.2, the popular transparent window types include single glazing, double glazing, vacuum glazing, and ventilation glazing. The structure and working principles of these windows, when integrated with hydrogel TC glass, are illustrated in Fig. 2. As shown in Fig. 2 (a), single glazing consists of only a single TC glass unit, with components arranged from outside to inside as follows: outer substrate glass, hydrogel, and inner substrate glass. In this configuration, the TC glass is in direct contact with indoor air, facilitating heat exchange through radiation and convection. For double glazing, as indicated in Fig. 2 (b), there is an air gap between the TC glass and the inner glass to minimize heat transmission between indoors and outdoors. Heat transfer in this case occurs via convection in the air gap and radiation between the TC glass and the inner glass. To further enhance thermal insulation, vacuum glazing replaces the air gap with the vacuum gap, as shown in Fig. 2 (c). This significantly reduces convective heat transfer between the TC and inner glass. To prevent glass deflection due to atmospheric pressure, an array of support pillars is arranged within the vacuum gap. Ventilation glazing differs from double glazing by incorporating the ventilation cavity in place of the air gap. As depicted in Fig. 2 (d), the upper end of the outer pane is equipped with an air outlet, while the lower end of the inner pane features an air inlet. This configuration allows for the exhaust of indoor air through the ventilation cavity, driven by fans. The cooling effect from the indoor exhaust air helps maintain the temperature of the inner glass close to room temperature, thereby reducing indoor heat gain and enhancing thermal comfort. The specific parameters of the studied windows, apart from length and width, are listed in Table 1. In this study, the thicknesses of the hydrogel layer and substrate glass for the hydrogel TC glass are set to 1 mm and 3 mm, respectively [46]. In modern buildings, the low-e glass is commonly used as the inner glass of multi-layer windows to reduce energy consumption [58]. In this study, a 3 mm low-e glass, identified as number 2031 in the International Glass Database (IGDB) [59], is

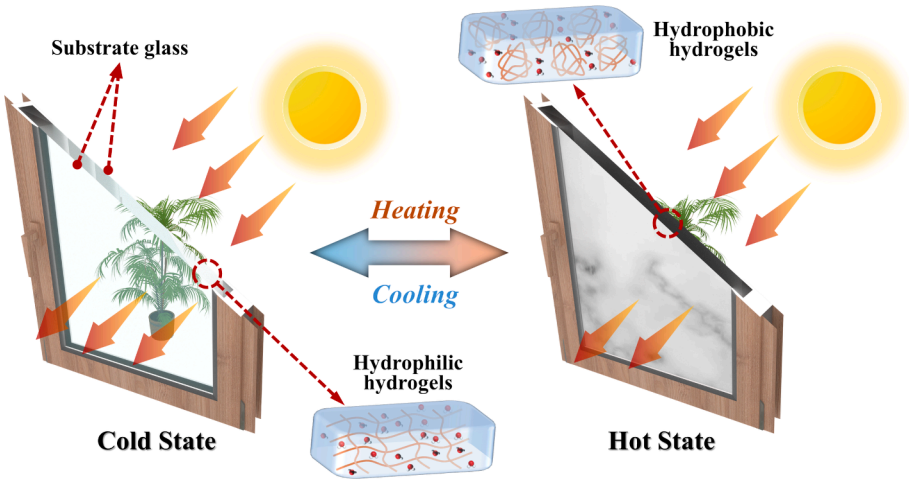

Fig. 1. The working principle of hydrogel-based thermochromic windows.

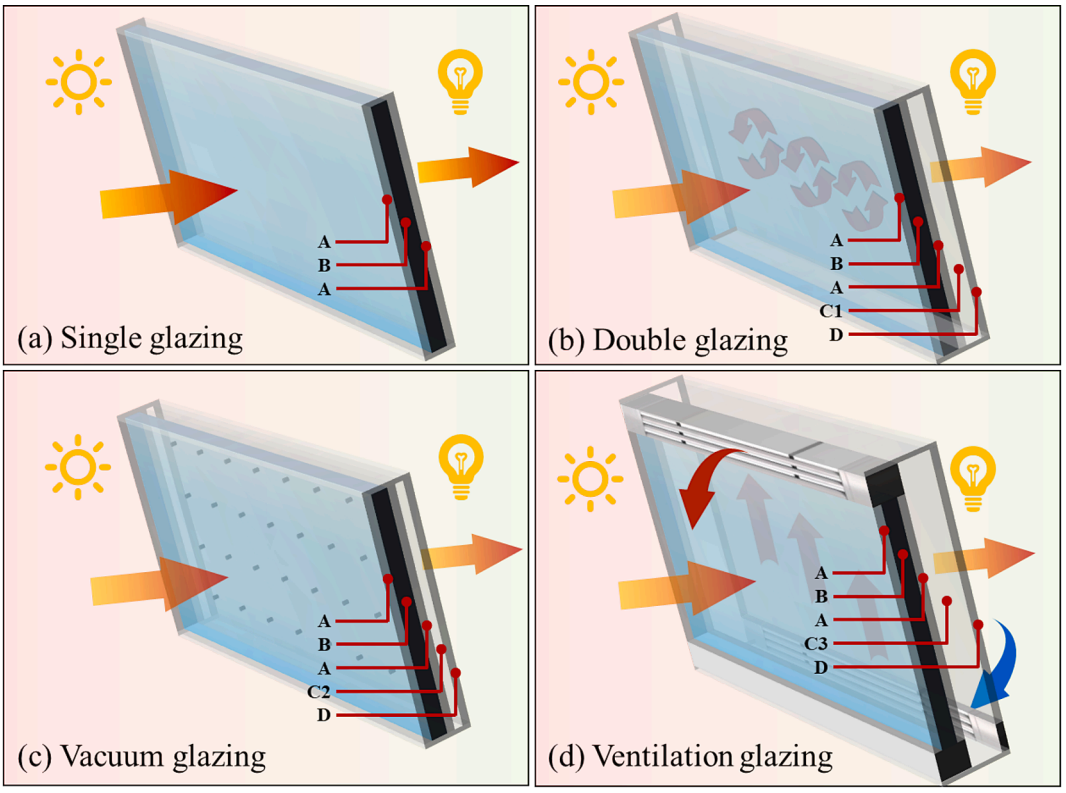

Fig. 2. The structure and working principle of various hydrogel-based thermochromic windows.

Table 1
The specific parameters of the studied windows.

Parameters		Values
Thickness	Substrate glass	3 mm [46]
	Hydrogel layer	1 mm [46]
	Air gap	12 mm [60]
	Vacuum gap	0.5 mm [63]
	Ventilation cavity	100 mm [61]
Inner glass		ID 2031 in IGDB [59]
Airflow rate of ventilation glazing		1 m/s [62]
Air pressure in vacuum gap		5×10^{-4} Pa [63]
Space and radius support pillars		35 mm, 0.2 mm [63]

selected as the inner glass of the double, vacuum, and ventilation glazing. Consistent with existing studies, the air gap thickness for double glazing and the cavity thickness for ventilation glazing are set to 12 mm [60] and 100 mm [61], respectively, while the air flow rate for ventilation glazing is 1 m/s [62]. For vacuum glazing, the relevant parameters, including the support pillars with a radius of 0.2 mm, a spacing of 35 mm, the vacuum gap with a thickness of 0.5 mm and an air pressure of 5×10^{-4} Pa, are obtained from a commercial vacuum window product [63].

As shown in Figs. 1-2, the most common configuration for hydrogel TC glass is a sandwich structure [64], where the TC hydrogel is enclosed between substrate glass. The optical properties of substrate glass in the solar spectrum significantly impact the performance of hydrogel-based

thermochromic windows. Moreover, the optical properties of substrate glass in the visible and near-infrared bands affect the building performance of TC glazed facades in different ways and should be analyzed separately. This study examines the impact of these optical properties on the overall performance of various hydrogel-based TC windows. Most types of commercial glass on the market are made of silica, and in their uncoated state, they have a similar refractive index. In this study, it was assumed a constant refractive index of 1.5 for the substrate glass of TC glass [46]. The extinction coefficients in the visible and near-infrared bands vary from 5 m^{-1} to 255 m^{-1} in intervals of 50 m^{-1}, covering the transmittance range of most glass available in IGDB, from clear to tinted [59].

3. Research methodology

3.1. Fabrication and characterization of hydrogel thermochromic glass

To obtain the comprehensive information on the hydrogel TC material, the hydrogel-based TC glass was fabricated by the authors, and its characteristic parameters were measured. The poly(NIPAM) hydrogel used in this study was prepared via the method in Ref [14]. First, 1.6 g of N-isopropyl acrylamide (NIPAM, 99 %, Sigma-Aldrich) was dissolved in 7 ml of deionized water and stirred until completely dissolved. Then, 5 mg of ammonium persulfate (APS, >98 %, Sigma-Aldrich) and 5.44 mg of methylene bisacrylamide (MBA, 99 %, Sigma-Aldrich) were added to the monomer solution and stirred until dissolved. Next, the precursor solution was synthesized by adding 3 mg of Na_2HSO_3 into the prepared liquid. This solution was then injected into the 1 mm gap between two pieces of 1 mm ultra-high transparency glass and sealed with UV-curing glue on all sides. Free radical polymerization was initiated at 25 °C for 15 min. Following this process, the hydrogel-based TC glass was successfully fabricated. As shown in Fig. 3 (a), the TC glass was transparent like water in its cool state and translucent like milk in its hot state.

The spectral transmittance/reflectance of the hydrogel-based TC glass in the wavelength range of 0.3–2.5 μm was measured using the UV–visible-near-infrared spectrophotometer (SHIMADZU UV3600), and the results are shown in Fig. 3(b). The solar and visible optical properties, modulation ability, and haze of the fabricated TC glass were calculated according to the equations in Table 2. The corresponding calculated results of the above indicators are listed in Table 3. The haze measurements showed the haze of the hydrogel in the hot state to be around 98 %, and close to 0 % in the cold state. Therefore, in this study, the hydrogel is considered a specular component in the cold state and an isotropic diffuse component in the hot state, which aligns with the conclusions of Wu et al. [46]. This conclusion and the optical parameters in the solar and visible bands will be used in the optical model of the TC glass in Section 3.2.1. Additionally, after repeated heating and cooling, it was observed that the transition temperature of the prepared hydrogel was around 32 °C.

Table 2
The calculation methods of performance metrics of the TC glass [7].

Metrics	Equations
Solar transmittance/reflectance	$Y_{sol} = \int_{0.3um}^{2.5um} \varphi(\lambda)Y(\lambda)d\lambda / \int_{0.3um}^{2.5um} \varphi(\lambda)d\lambda$
Visible transmittance/reflectance	$Y_{vis} = \int_{0.38um}^{0.78um} \phi(\lambda)Y(\lambda)d\lambda / \int_{0.38um}^{0.78um} \phi(\lambda)d\lambda$
Solar modulation ability	$\Delta T_{sol} = T_{sol}^{cold} - T_{sol}^{hot}$
Haze	$Haze = \frac{T_4}{T_2} - \frac{T_3}{T_1}$

Table 3
The optical properties of the fabricated TC glass.

States	Solar transmittance	Visible transmittance	Haze	Solar modulation ability
Cold	0.82	0.90	0	0.61
Hot	0.21	0.22	0.98	

In the table, Y represents the optical properties, such as transmittance T or reflectance R; λ is the wavelength (um). φ is the solar irradiance spectrum of air mass 1.5 (W • m^{-2} • um^{-1}); ϕ is the CIE photopic luminous efficiency of the human eye; T_1 and T_2 are the total transmittance of the air and sample while T_3 and T_4 are the diffuse transmittance of the air and sample. The specific details for haze measurement can be found in the ASTM D1003.

3.2. Modeling process and simulation setup

Considering the primary impact of TC windows on buildings, this study evaluated the hydrogel-based TC windows in terms of building energy consumption and indoor human comfort. EnergyPlus, a widely

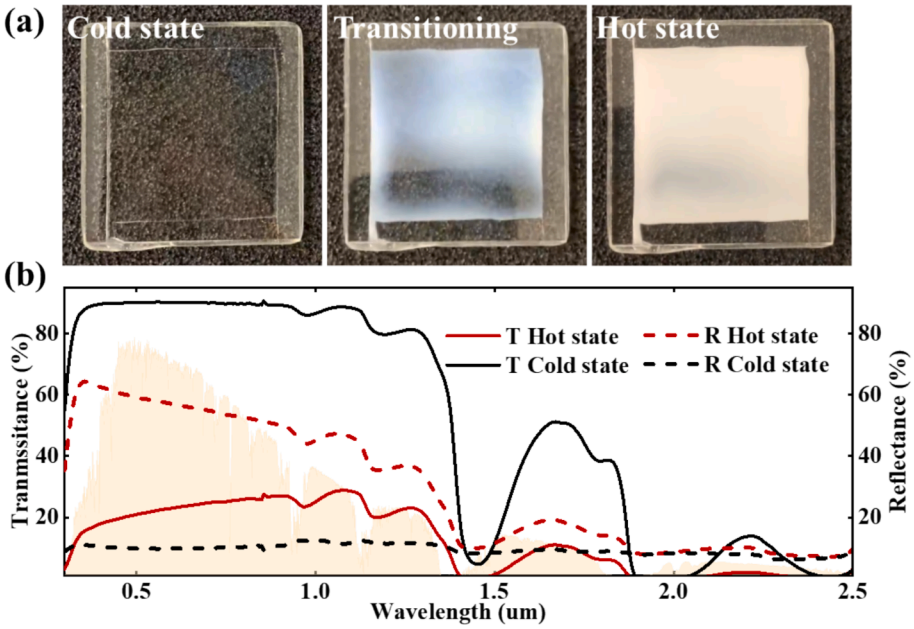

Fig. 3. The appearance and optical properties of fabricated hydrogel-based TC glass.

utilized building energy simulation tool in research and engineering fields, provides detailed computational models for predicting the energy performance of various window types as described in Section 2. These models for window calculations are sourced from ISO 15099 [65], a well-established standard with a strong validation history from a lot of studies [66–68]. Radiance software is recognized as the leading indoor illuminance environment calculation and rendering engine based on the Monte Carlo backward ray-tracing algorithm. It is extensively employed in simulating indoor natural daylighting for windows, shading, and complex fenestration systems. Its high precision has also been widely confirmed in previous studies [69,70]. In relatively stable indoor thermal environments such as air-conditioned rooms, Fanger's PMV-PPD model is typically more suitable for predicting thermal comfort [71]. Ladybug software incorporates this model based on the standard calculation model in ISO 7730 [72]. Therefore, for this study, the aforementioned three software tools were selected to assess energy performance, visual comfort, and thermal comfort, respectively.

The research flowchart for optimization and performance evaluation is depicted in Fig. 4. Initially, the optical data of the hydrogel glass with various substrate glass in both hot and cold states were computed using Matlab, based on the optical model outlined in Section 3.2.1. Subsequently, the optical characteristics of the hydrogel glass in hot and cold states, along with the inner glass, were input into the WINDOW software to configure the studied windows as per the parameters specified in Table 1. The resulting IDF files, containing structural details and optical properties, were then generated. Then, these IDF files were transferred to EnergyPlus for the computation of cooling loads, while the visible properties of the studied windows were imported into Radiance for the assessment of visual comfort and indoor illuminance. The transition state of the TC glass (hot or cold state) in EnergyPlus was automatically switched by the EMS object based on the TC glass temperature, and the transition states from EnergyPlus were utilized to adjust the optical parameters in Radiance calculations. The EMS object in EnergyPlus can adjust the optical parameters of glass during simulation based on the signal stimulus, such as the temperature of TC glass in this study. It is commonly utilized in building simulation involving thermochromic glass [33,46,49]. Finally, the indoor illuminance calculated by Radiance was imported into EnergyPlus to determine artificial lighting loads. The indoor operative temperature and humidity data from EnergyPlus were imported into Ladybug to predict thermal comfort. The parameter settings used in these simulation tools are detailed in Section 3.2.2. Data transmission between different simulation tools was facilitated by the Grasshopper platform. After all calculations were completed, the metrics related to energy consumption and indoor comfort, as described in Section 3.3, were collected and comprehensively analyzed. Before conducting the simulation, this study calibrated the accuracy of the simulation tools used as well as the state-switching approach of TC glass via EMS, by validating the simulation method against reference data. The detailed validation process is presented in Appendix A.

3.2.1. Optical model of thermochromic glass

In this study, the optical properties of hydrogel glass with different substrate glass are determined using the net radiation method. This recursive method accounts for the infinite refraction and reflection of rays in multiple layers of a medium. It is a widely used mathematical model for calculating multi-layer glass systems and is included in ISO 15099, as well as utilized by multiple architectural glass simulation tools such as Optics, WINDOW, and EnergyPlus. As shown in Fig. 5, the hydrogel-based thermochromic windows include four interfaces (numbered in the figure) and three medium layers (substrate glass, hydrogel, and substrate glass). The equations for the net radiation method in both the cold and hot states are presented below. It is important to note that all variables in these equations are dimensionless parameters.

When the hydrogel is in cold state, the three layers in the glass are specular layers, meaning there are no diffuse rays inside the mediums. The overall transmittance and reflectance of the hydrogel TC glass are calculated by:

$$T^{f}_{1,4} = \frac{T^{f}_{1,3}\tau_g{}^{beam}(1 - r_4{}^{beam})}{1 - r_4{}^{beam}\tau_g{}^{beam}R^{b}_{1,3}} \tag{1}$$

$$R^{f}_{1,4} = R^{b}_{1,4} = R^{f}_{1,3} + \frac{T^{f}_{1,3}(\tau_g{}^{beam})^2 r_4{}^{beam}T^{b}_{1,3}}{1 - r_4{}^{beam}(\tau_g{}^{beam})^2 R^{b}_{1,3}} \tag{2}$$

where, τ_g is the transmissivity in substrate glass interior. r_4 is the reflectivity at interface 4, which is the boundary between the glass and air. $T^{f}_{1,3}$ and $T^{b}_{1,3}$ are the front and back transmittance of sub glazing between interface 1 and 3. $R^{b}_{1,3}$ and $R^{b}_{1,3}$ are the front and back reflectance of the sub glazing between interface 1 and 3. Similarly, they are calculated as:

$$T^{f}_{1,3} = T^{b}_{1,3} = \frac{(1 - r_1{}^{beam})\tau_g{}^{beam}T^{c}_{2,3}}{1 - R^{c}_{2,3}(\tau_g{}^{beam})^2 r_1{}^{beam}} \tag{3}$$

$$R^{f}_{1,3} = r_1{}^{beam} + \frac{(1 - r_1{}^{beam})^2(\tau_g{}^{beam})^2 R^{c}_{2,3}}{1 - r_1{}^{beam}(\tau_g{}^{beam})^2 R^{c}_{2,3}} \tag{4}$$

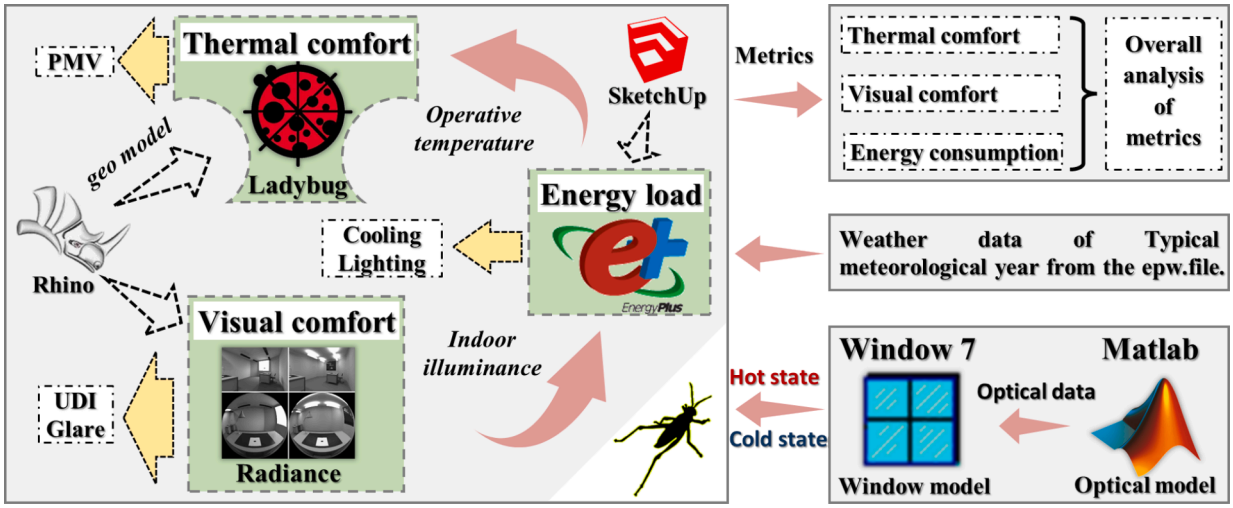

Fig. 4. The research flowchart for optimization and performance evaluation.

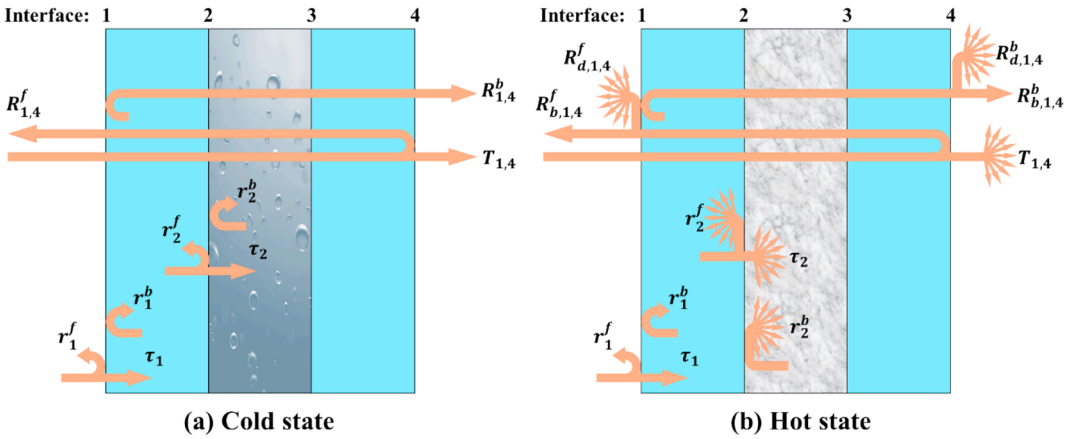

Fig. 5. Schematic diagrams illustrating the optical calculation.

$$R^b_{1,3} = R^c_{2,3} + \frac{{T^c_{2,3}}^2 ({\tau_g}^{beam})^2 {r_1}^{beam}}{1 - {r_1}^{beam} ({\tau_g}^{beam})^2 R^c_{2,3}} \tag{5}$$

where, $T^c_{2,3}$ and $R^c_{2,3}$ are the transmittance and reflectance of the hydrogel layer in the cold state. Since the medium on both sides of the hydrogel is the same, the front and back transmittance/ reflectance are also the same. r_1 represents the reflectivity at interface 1, which is also the boundary between the glass and air.

When the hydrogel is in its hot state, the hydrogel layer in the glass becomes a scattering layer. All rays passing through or being reflected from this layer are completely scattered. As shown in Fig. 5 (b), notably, all rays passing through the hydrogel-based glass are scattered, while the reflected rays consist of both diffuse and beam irradiation. The overall transmittance and reflectance of the hydrogel-based glass are calculated by:

$$T^f_{1,4} = \frac{T^f_{1,3} {\tau_g}^{dif} (1 - {r_4}^{dif})}{1 - {r_4}^{dif} {\tau_g}^{dif} R^b_{1,3}} \tag{6}$$

$${R^f_{1,4}}^{dif} = {R^b_{1,4}}^{dif} = {R^f_{1,3}}^{dif} + \frac{T^f_{1,3} ({\tau_g}^{dif})^2 {r_4}^{dif} T^b_{1,3}}{1 - {r_4}^{dif} ({\tau_g}^{dif})^2 R^b_{1,3}} \tag{7}$$

$${R^f_{1,4}}^{beam} = {R^b_{1,4}}^{beam} = {R^f_{1,3}}^{beam} \tag{8}$$

where, the superscript '*beam*' represents beam irradiation, and '*dif*' denotes diffuse irradiation. $T^f_{1,3}$, $T^b_{1,3}$, and $R^b_{1,3}$ are only diffuse irradiation, so they are not distinguished by superscripts.

$$T^f_{1,3} = \frac{(1 - {r_1}^{beam}) {\tau_g}^{beam} T^h_{2,3}}{1 - R^h_{2,3} ({\tau_g}^{dif})^2 {r_1}^{dif}} \tag{9}$$

$$T^b_{1,3} = \frac{T^h_{2,3} {\tau_g}^{dif} (1 - {r_1}^{dif})}{1 - {r_1}^{dif^2} {\tau_g}^{dif} R^h_{2,3}} \tag{10}$$

$${R^f_{1,3}}^{beam} = {r_1}^{beam} \tag{11}$$

$${R^f_{1,3}}^{dif} = \frac{(1 - {r_1}^{beam}) {\tau_g}^{beam} R^h_{2,3} {\tau_g}^{dif} (1 - {r_1}^{dif})}{1 - {r_1}^{dif} ({\tau_g}^{dif})^2 R^h_{2,3}} \tag{12}$$

$$R^b_{1,3} = R^h_{2,3} + \frac{{T^h_{2,3}}^2 ({\tau_g}^{dif})^2 {r_1}^{dif}}{1 - {r_1}^{dif} ({\tau_g}^{dif})^2 R^h_{2,3}} \tag{13}$$

where, $T^h_{2,3}$ and $R^h_{2,3}$ are the transmittance and reflectance of the hydrogel layer in the hot state.

The transmittance and reflectance of the hydrogel layer in both cold and hot states are obtained through experimental measurements as detailed in Section 3.1. The transmissivity τ_g and reflectivity r of the substrate glass are calculated by substituting the refractive index and extinction coefficient into the Bouguer's law and Fresnel's law equations as described in Ref [73]. The properties of beam irradiation are calculated using these laws for non-normal incidence, while the properties of diffuse irradiation are determined through numerical integration of the calculations over the hemisphere. Before calculating the optical data of hydrogel glass with different substrate glass, the above equations were calibrated using reference data. The validation process of the optical model employed in this study is detailed in Appendix B.

3.2.2. *Assessment models of energy·and human comfort*

Generally, TC glass is mainly suitable for cooling-dominated regions [45]. In this study, the building energy consumption and indoor human comfort of the studied thermochromic glazing were evaluated using a case study of an office building in Shenzhen, China. As illustrated in Fig. 6, the building measures 5 m in width, 5 m in length, and 3 m in height. It features a window measuring 4 m in width and 2 m in height installed on the south wall. It was assumed that the indoor occupancy is 5 m^2/person and the occupancy time for the office spans from 8:00 am to 6:00 pm. The materials and thermophysical properties of the building envelopes are detailed in Table 4. During the calculation, the vertical walls conduct the heat transfer to outdoors, and the floor/ceiling is set as the internal wall, which exchanges heat with the adjacent rooms. Weather data from a typical meteorological year in Shenzhen were used as boundary conditions for year-round simulations. Shenzhen, located in the southern part of China (22.55 N, 114.1 E), typifies a region characterized by hot summers and warm winters. Therefore, in this study, heating energy consumption is not considered as there is almost no heating demand in the studied area. The ambient temperature and solar irradiation in Shenzhen are shown in Fig. 6 (c) and (d). The monthly average temperature ranges from 15 °C to 28 °C throughout the year. Solar irradiation varies between 50 kWh/m^2 and 100 kWh/m^2, with the minimum occurring in May and June and the maximum in December.

The data in the table are acquired from the building library of the Commercial Reference Buildings developed by the U.S. Department of Energy [74].

The daylighting model for evaluating visual comfort and indoor illuminance was developed in Radiance software. The Honeybee plugin in Grasshopper can activate Radiance software and process the parameter settings. In accordance with a previous study [75], the parameters in the software including ambient bounces(−ab), ambient divisions (−ad), ambient super-samples (−as), ambient resolution (−ar), and ambient accuracy (−aa) were set to 10, 1024, 2, 96, and 0.15, respectively. This parameter setup aims to optimize time efficiency without

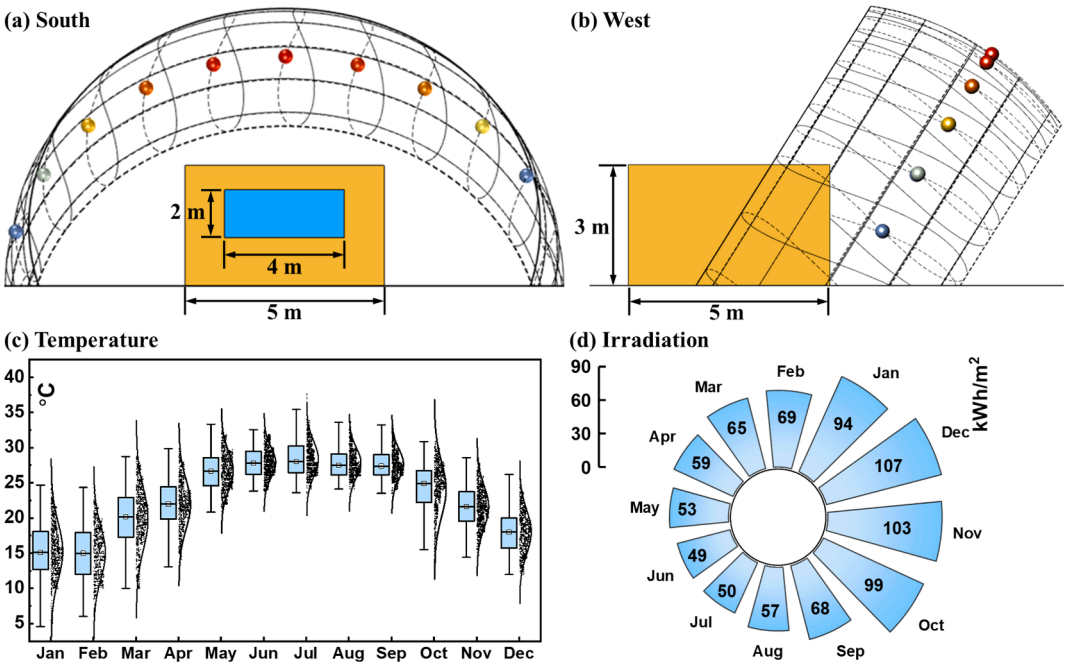

Fig. 6. The building model and weather parameters in the case study.

Table 4
The materials and thermophysical properties of the building envelope.

	Material	Thickness (m)	Conductivity (W/m • K)	Density (W/m^3)	Specific heat (J/kg • K)	R-value (m^2 • K/W)
Wall	Stucco	0.025	0.72	1856	840	/
	Gypsum board	0.016	0.16	800	1090	/
	Concrete block	0.20	1.32	1842	912	/
	Insulation layer	/	/	/	/	0.77
	Gypsum board	0.016	0.16	800	1090	/
Floor	Concrete block	0.15	1.32	1842	912	/
	Insulation layer	/	/	/	/	0.21
Ceiling	Insulation layer	/	/	/	/	0.21
	Concrete block	0.15	1.32	1842	912	/

compromising calculation accuracy. The illuminance on the indoor work plane, a horizontal surface positioned 1 m above the floor was calculated to assess indoor daylighting performance [76]. The thermal comfort was predicted according to the model in the Ladybug software. After the indoor thermal conditions, including air temperature, mean radiant temperature, and relative humidity, calculated in EnergyPlus software were input, the Ladybug software employs the PMV-PPD model to evaluate the indoor thermal comfort. This model calculates the predicted mean vote (PMV) and predicted percentage of dissatisfied (PPD) occupants, considering various factors including metabolic activity, clothing, and environmental conditions, among others. Following the guideline outlined in ASHRAE 55 [77], the parameters utilized to assess indoor thermal comfort encompass clothing insulation values of 0.5 clo under hot conditions and 1.0 clo under cold conditions. This methodology acknowledges the potential for individuals to adjust their clothing in response to thermal discomfort. Additional parameters employed in the calculation include an air velocity of 0.1 m/s and a metabolic rate of 1.1 met, representative of a sedentary human occupant.

The heat transfer and energy performance of the studied building was predicted by EnergyPlus software. As described above, only cooling load is considered in the case study. In accordance with local government standards GB 50736–2012 [78], the cooling set temperature was established at 24℃. This setting mandates that the building's air conditioning operates during the occupied time to maintain the indoor temperature below the specified set point. It was assumed that an air source heat pump was used to convert the cooling load to the electricity consumption for cooling. According to the GB 19576–2019 [79], the rate performance coefficient of the heat pump was assumed to be 2.8. The minimum illuminance on the work plane, obtained from Radiance software, was imported into EnergyPlus for calculating lighting load. In this study, the on/off control method was employed, which means that once the minimum illuminance of the work plane is lower than the required value, the lamp will be turned on at full power. As stipulated by GB 50033–2013 [80], the artificial lighting density in this study was 9 W/m^2, with a required minimum illuminance of 450 lx.

3.3. Evaluation metrics

The energy performance is evaluated by summing electricity use for cooling and lighting during the annual occupancy time according to the method in Section 3.2.2. To assess visual comfort across the entire work plane, the metric of spatial Useful Daylight Illuminance (UDI) autonomy is used [50]. This metric represents the area ratio of the indoor work plane where the UDI exceeds 50 %. The UDI measures the percentage of annual occupy time when indoor illuminance at a specific location falls between the minimum required illuminance (450 lx in this study) and 2000 lx [76]. Illuminance values below 450 lx are too dim for human activity, while values above 2000 lx may cause glare. According to ASHRAE 55, indoor thermal conditions are considered neutral when the PMV values falls within the range of −0.5 to 0.5. A PMV value above 0.5

indicates hot conditions, while a PMV value below −0.5 indicates cold conditions. In this study, the thermal comfort performance of various types of TC windows was evaluated by the time percentage of thermal comfort, defined as the ratio of the time when indoor thermal sensation is neutral to the total occupancy time throughout the year.

4. Results

4.1. Sensitivity analysis of optical properties

This section analyzes the impact of the optical properties of substrate glass on the overall performance of TC windows. The primary objective is to elucidate the variation patterns in energy consumption, visual comfort, and thermal comfort, as well as to assess the sensitivity of these performance metrics to changes in the optical parameters of substrate glass. Throughout this analysis, the extinction coefficients of the substrate glass, except for the variables under examination, are maintained consistently at 5 m^{-1} for visible and near-infrared irradiation. The dependent variables analyzed, in addition to the evaluation metrics in Section 3.3, include the time percentage in hot state, which refers to the percentage of TC glass in hot state during the annual occupied time.

4.1.1. Visible properties of substrate glass

The impact of visible properties on the overall performance of various types of TC windows is shown in Fig. 7. Notably, the time percentage of TC glass in hot states increases with the rise in extinction coefficients. As the extinction coefficient increases from 5 m^{-1} to 255 m^{-1}, the time percentages in hot states for double and vacuum glazing exhibit similar changes, increasing by approximately 50 %, while single glazing shows a 47 % increase. Ventilation glazing displays the smallest change, only 34 %, primarily due to the cooling effect of airflow, which stabilizes the temperature of the hydrogel glass. The change in the transition states of hydrogel glass affects building energy consumption and human comfort. Cooling consumption decreases due to reduced indoor heat gain, while lighting consumption increases due to diminished indoor illuminance. Consequently, total electricity use first decreases and then increases, reaching a minimum when the extinction coefficients are between 55 and 155 m^{-1}. The spatial UDI autonomies of all windows follow similar trends, initially increasing and then decreasing. The maximum spatial UDI autonomy for double and vacuum glazing exceeds 90 % when the extinction coefficients are around 105 to 155 m^{-1}. For thermal comfort, the increase in visible absorbance has minimal impact on ventilation glazing due to its robust temperature regulation. However, the thermal comfort of single glazing declines sharply, from 55 % to 33 %, significantly more than other glazing types, attributed to the substantial temperature increase on the window inside.

4.1.2. Near-infrared properties of substrate glass

The impact of near-infrared properties on the overall performance of various types of windows is shown in Fig. 8. The increase in the extinction coefficient raises the time percentage in hot state. This increase is comparable to the results for visible properties because visible and near-infrared irradiation account for roughly equal proportions of the solar spectrum. Almost all the electricity used in this subsection is for cooling consumption, as the lighting load is nearly zero. As shown in Fig. 8 (b), the electricity use decreases with the increase in extinction coefficients. However, when the extinction coefficient reaches approximately 155 m^{-1}, the electricity use levels off with minimal variation. Thus, there is a limit to reduce energy consumption by increasing the near-infrared extinction coefficient. Regarding spatial UDI autonomy, the increase in the extinction coefficient consistently enhances the values for various TC windows. Therefore, increasing the near-infrared extinction coefficient always benefits visual comfort. For thermal comfort, the results are consistent with the analysis results of the visible properties. The indoor thermal comfort of single glazing diminishes, while other window types experience minimal effects.

4.1.3. Global analysis of visible and near infrared properties

This section analyzes the global impact of visible and near-infrared properties on the performance of hydrogel-based TC windows. After all optical parameters are arranged and combined, a total of 36 cases were examined, and their performance metrics are presented in Fig. 9. As illustrated in Fig. 9 (a), the transition states of double and vacuum glazing are generally higher than those of single glazing, while ventilation glazing exhibits the lowest transition state. Especially, when the visible and near-infrared extinction coefficients of the substrate glass are 5 m^{-1}, typically representing ultra-white glass, single glazing and ventilation glazing will not undergo significant state transitions. Fig. 9

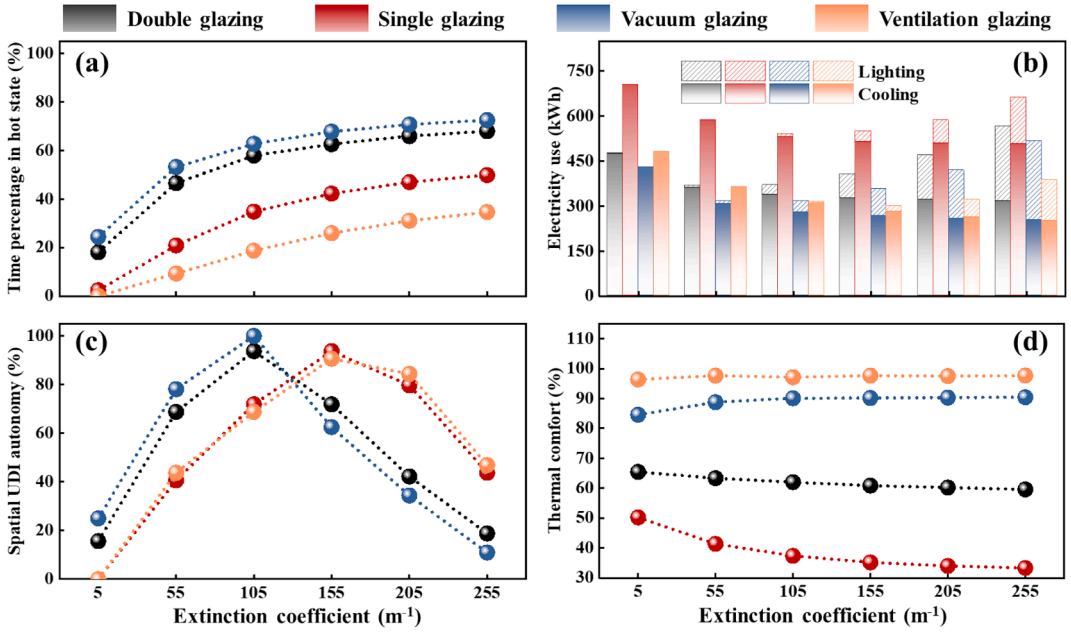

Fig. 7. The impact of visible properties on the overall performance: (a) Time percentage in hot state; (b) Electricity use; (c) Spatial UDI autonomy; (d) Time percentage of thermal comfort.

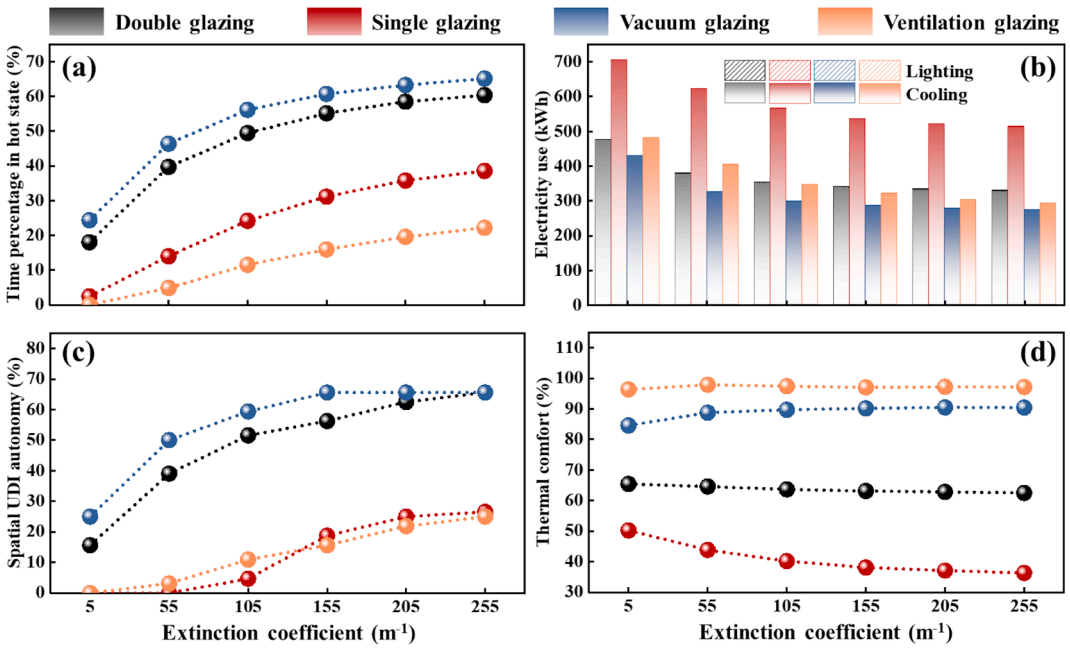

Fig. 8. The impact of near-infrared properties on the overall performance: (a) Time percentage in hot state; (b) Electricity use; (c) Spatial UDI autonomy; (d) Time percentage of thermal comfort.

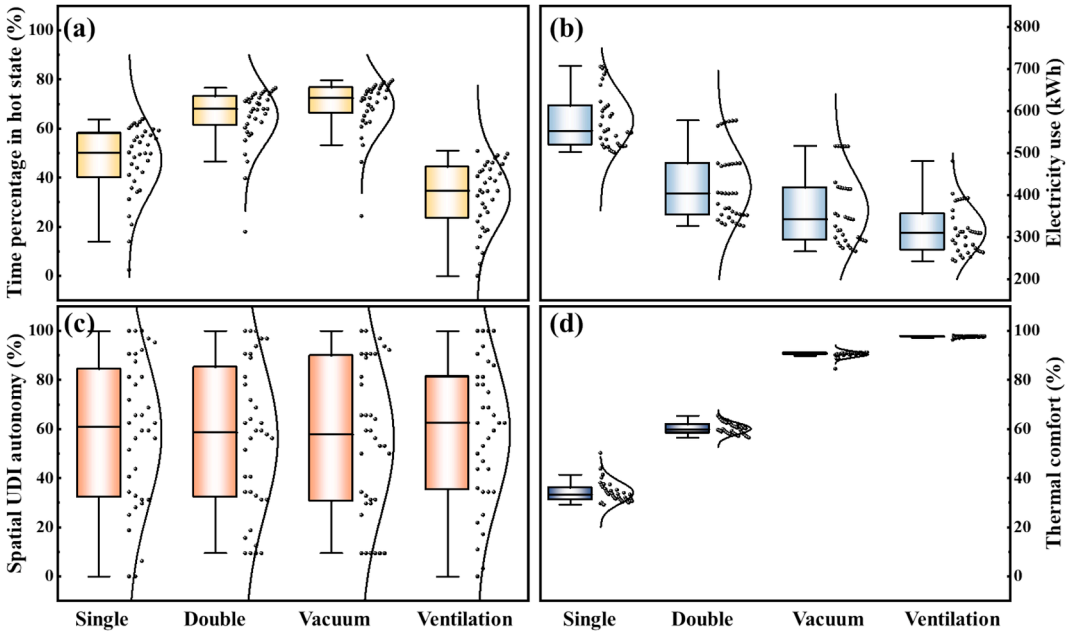

Fig. 9. The impact of near infrared properties on the overall performance: (a) Time percentage in hot state; (b) Electricity use; (c) Spatial UDI autonomy; (d) Time percentage of thermal comfort.

(b) illustrates the electricity consumption associated with various window types when employing different substrate glass. Notably, ventilation and vacuum glazing show the lowest energy consumption. Regarding visual comfort, all examined glazing types exhibit high sensitivity to the optical properties of substrate glass, with the spatial UDI autonomy varying between 0 % and 100 %. Conversely, the thermal comfort levels of different glazing types show considerable variability in their sensitivity to substrate glass. For vacuum and ventilation glazing, the time percentage of acceptable thermal comfort remains consistently high at approximately 90 % and 97 %, respectively. The thermal comfort of single and double glazing varies between 30–50 % and 55–65 %, respectively.

By analyzing and comparing the various performance metrics of windows with different substrate glass configurations, the optimal optical properties for each window type were identified. In this study, the optical parameters are deemed optimal when the thermal and visual comfort metrics exceed the median values of all cases, while simultaneously minimizing energy consumption. For double and vacuum glazing, the lowest energy consumption occurred when the visible irradiation extinction coefficient was set at 55 m^{-1} and the near-infrared extinction coefficient ranged from 155 to 255 m^{-1}. In addition, the spatial UDI autonomy exceeded 90 %, and thermal comfort remained above the median level. Consequently, these extinction coefficients for double and vacuum glazing were determined to be optimal optical

properties. For single and ventilation glazing, the analysis revealed that a visible irradiation extinction coefficient of 105 m^{-1} and a near-infrared extinction coefficient of 155 to 255 m^{-1} resulted in the lowest energy consumption, while the metrics for visual and thermal comfort exceeded the median values across all cases. Therefore, these values were chosen as the optimal properties for single glazing.

4.2. Overall performance of different types of windows

In this section, the overall performance of various window types is compared. To ensure a fair comparison, all studied windows utilize the substrate glass with identical optical parameters. The analysis in Section 4.1.3 reveals that the optimal extinction coefficients for the windows range from 55 to 105 m^{-1} for visible irradiation and from 155 to 255 m^{-1} for near-infrared irradiation. Therefore, an average optical coefficient of 80 m^{-1} for visible irradiation and 205 m^{-1} for near-infrared irradiation was selected for the analysis. Additionally, to underscore the enhanced performance resulting from retrofitting with hydrogel-based glass, the single, double, vacuum, and ventilation types of clear windows constructed with ultra-clear glass (extinction coefficient of 5 m^{-1}) as the outer layer were compared as a baseline.

Before analyzing the various evaluation metrics, the temperature of the hydrogel glass under annual outdoor weather conditions was summarized and compared, as shown in Fig. 10. The results indicate that the glass temperature is highly dependent on incident solar radiation and ambient temperature. Under identical environmental conditions, vacuum glazing exhibits the highest temperature, followed by double glazing, single glazing, and ventilation glazing, which records the lowest temperature. This trend can be attributed to the superior thermal insulation properties of vacuum glazing, which effectively minimizes heat exchange between the hydrogel glass and the interior environment. In contrast, single glazing facilitates direct heat exchange with the indoor environment, resulting in lower temperatures. Additionally, for ventilation glazing, the airflow within the air gap cools the hydrogel glass, contributing to its lower temperature compared to other window types. Overall, the percentages of time during which the temperature exceeds the transition temperature of the hydrogels are 52 %, 69 %, 73 %, and 37 %, respectively. Notably, the use of standard hydrogel glass in single and ventilation glazing results in minimal state transitions, underscoring the necessity for optimizing the optical properties of the substrate glass.

4.2.1. Energy consumption

To reveal the causes of the impact of various windows on indoor energy consumption, the heat gain of various windows on a typical sunny summer day, August 14th of a typical meteorological year, was first analyzed, as shown in Fig. 11. The convection and radiation heat transfer through the windows, termed secondary heat gain, depends on the temperature difference between the inner glass and the indoors. As depicted in Fig. 11 (a) and (b), the ventilation glazing exhibits the lowest secondary heat gain, followed by vacuum glazing and double glazing, while single glazing demonstrates the highest heat transfer. The superior performance of ventilation glazing in reducing secondary heat gain is primarily attributed to the cooling effect of the airflow, which brings the temperature of the inner glass very close to room temperature. Notably, the convection heat transfer of ventilation glazing is nearly 0 W, while the radiation heat transfer is negative, reaching a minimum of −50 W. The transmitted irradiation, referred to as direct heat gain, mainly depends on the transition states. The direct heat gain of vacuum glazing is the lowest due to the extended periods of hot states. Summing these factors, the net heat transfer profiles of various windows are depicted in Fig. 11 (d). The heat gain of vacuum glazing is the lowest, closely followed by double glazing, while the heat gain of single glazing is the highest.

The monthly electricity use of various hydrogel-based TC windows and their corresponding clear windows is shown in Fig. 12. The building's electricity use is highest from June to September and lowest from January to March, a trend driven by local climate conditions. As expected, the monthly electricity use for single glazing, whether TC or clear windows, is consistently the highest due to the greater heat gain, as explained in Fig. 11. Among the four window types, ventilation glazing

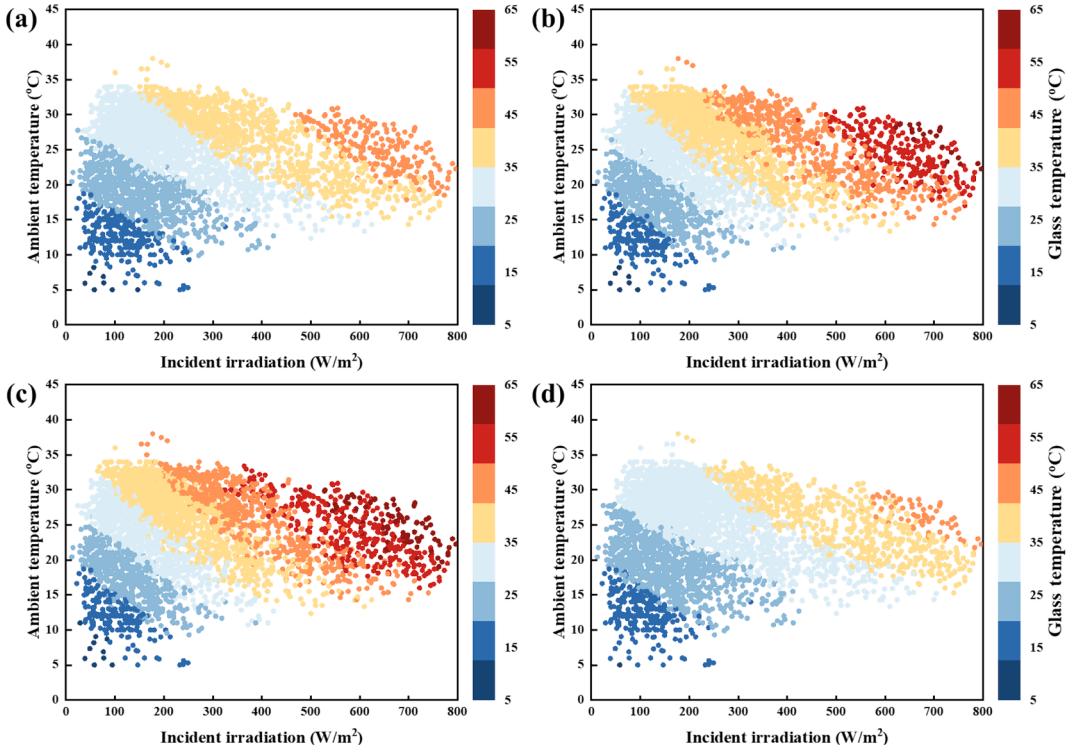

Fig. 10. Temperature of hydrogel glass under annual outdoor weather parameters: (a) Single glazing; (b) Double glazing; (c) Vacuum glazing; (d) Ventilation glazing.

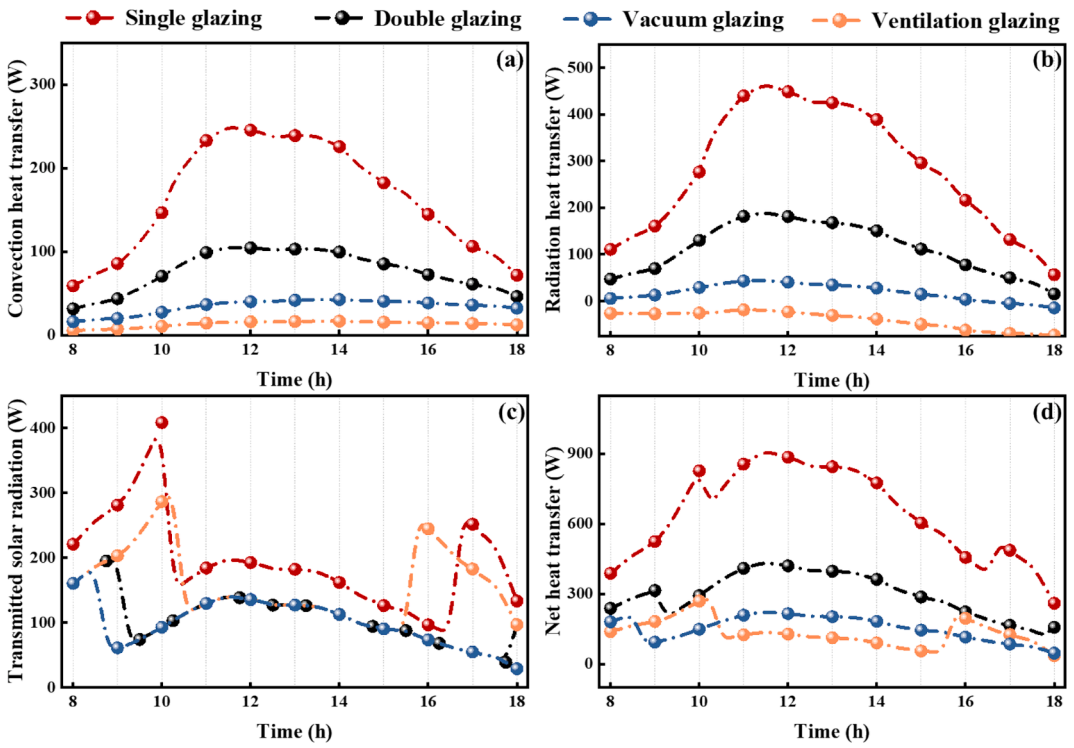

Fig. 11. Heat transfer through various windows in a typical day: (a) Convection heat transfer; (b) Radiation heat transfer; (c) Transmitted solar irradiation; (d) Net heat transfer.

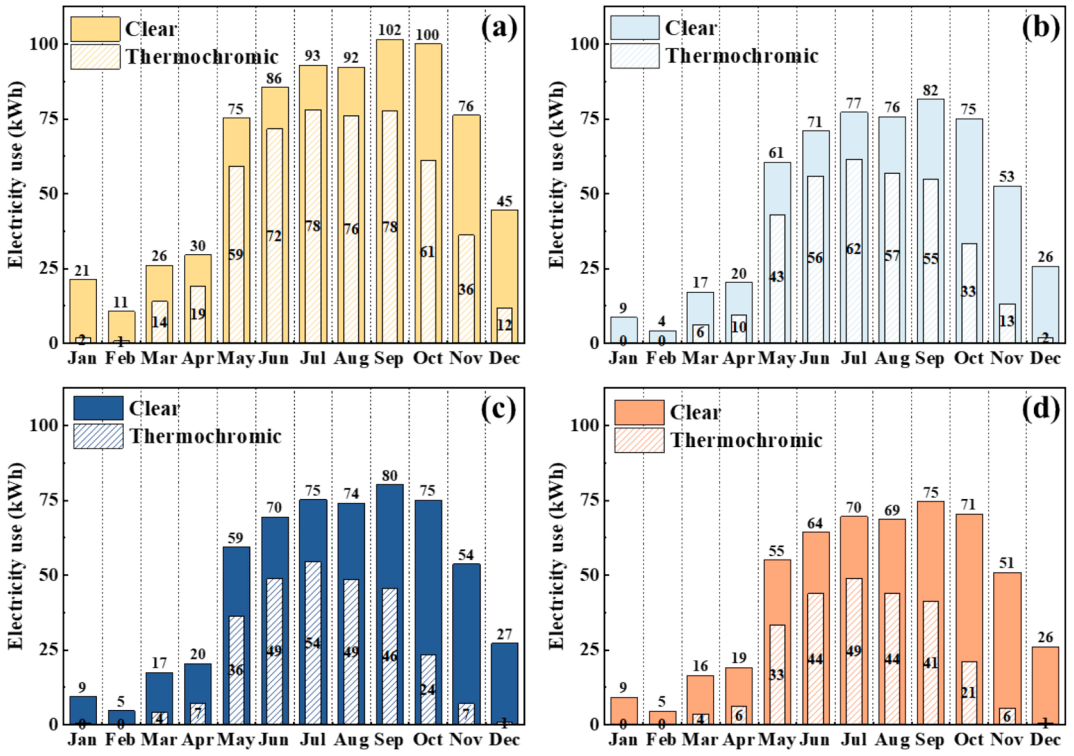

Fig. 12. The electricity use of various hydrogel-based thermochromic windows: (a) Single glazing; (b) Double glazing; (c) Vacuum glazing; (d) Ventilation glazing.

demonstrates the most significant energy-saving effect. Summing the annual data, the electricity use of the studied TC windows for single, double, vacuum, and ventilation glazing is 507 kWh, 337 kWh, 277 kWh, and 248 kWh, respectively. Comparing TC and clear windows, it was found that TC glass can reduce energy consumption for all window types. Among them, TC glass has the most pronounced energy-saving effect on vacuum and ventilation windows, achieving a reduction of 289 kWh and 281 kWh in electricity use. Single glazing follows with reductions of 249 kWh while double glazing has the least consumption reduction effect, at only 233 kWh. The energy saving ratios for these

windows after implementing the TC glass are 33 %, 41 %, 51 %, and 53 %, respectively.

4.2.2. Thermal comfort

The indoor thermal conditions presented on the psychrometric chart throughout the year are shown in Fig. 13. In this figure, the grid within the black frame indicates the indoor conditions that meet acceptable thermal comfort standards. Notably, the thermal comfort of single glazing is significantly reduced when the outer glass is replaced with hydrogel glass, with the time percentage of thermal comfort decreasing from 55.2 % to 32.9 %. The elevated temperature of the hydrogel glass increases the perceived temperature for occupants, resulting in 60 % of the occupied time being classified as the hot conditions. Similarly, the thermal comfort of double glazing shows a slight decrease after substituting the outer glass with hydrogel glass. However, this effect is less pronounced due to the heat transfer barrier provided by the inner glass. In contrast, the indoor thermal comfort of vacuum and ventilation glazing improves by 19.3 % and 2.8 %, respectively, after the outer layer is replaced with hydrogel glass. The improvement in thermal comfort for ventilation glazing is almost negligible, whereas the enhancement for vacuum glazing is significant. This improvement can be attributed to the hydrogel glass blocking solar irradiation, thereby reducing the temperature of the interior surfaces of walls. The comparison among various window types indicates that ventilation glazing consistently offers the best thermal comfort, followed by vacuum glazing, double glazing, and finally single glazing.

To further elucidate the observed changes in indoor thermal comfort, the distribution of indoor operative temperature during the annual simulation is presented in Fig. 14. Generally, indoor conditions are considered hot when the operative temperature exceeds 26 °C. For hydrogel-based single glazing, the probability density functions (PDFs) for the temperature ranges of 26–27 °C, 27–28 °C, and 28–29 °C are 20.9 %, 25.1 %, and 9.0 %, respectively, indicating poor thermal comfort. A similar phenomenon is observed with double glazing, where the PDF for the 26–27 °C range increases from 16.3 % to 23.0 % when using hydrogel glass. In the case of vacuum glazing, the PDF for the 26–27 °C range is 0 % for the thermochromic window and 11.4 % for the clear window. For ventilation glazing, the PDF for temperatures exceeding 26 °C remains at 0 %, regardless of the installation of hydrogel glass.

4.2.3. Visual comfort

The distribution of indoor Useful Daylight Illuminance (UDI) on the work plane is presented in Fig. 15. Notably, the UDIs at each position on the indoor work plane show significant improvement after the installation of hydrogel glass. For clear windows, the UDI values range from 0 % to 40 %, with lower values observed near the windows and higher values further away. The spatial UDI autonomies for all studied windows are 0 %, as transparent glass tends to result in indoor illuminance exceeding 2000 lx, which does not meet human visual needs and may lead to glare. In contrast, the use of TC glass markedly enhances the UDI on the interior work surface, attributable to the shading effect produced by the hot states of the hydrogel glass. Upon calculation, the spatial UDI autonomies for single, double, vacuum, and ventilation glazing are 78 %, 96 %, 100 %, and 72 %, respectively. The UDI values for single and ventilation glazing remain relatively low due to the shorter duration of hot states.

As indicated above, the higher indoor illuminance associated with clear windows may result in glare. To further evaluate indoor visual comfort, this subsection employs the Daylight Glare Possibility (DGP) metric, produced by Radiance software, to assess the extent of indoor glare [58]. Generally, a DGP value of less than 0.4 is considered acceptable for human comfort. The results of the probability density function (PDF) and cumulative distribution function (CDF) are presented in Fig. 16. Notably, the distribution of DGP values is concentrated in the range of 0.2–0.5 for thermochromic windows and 0.4–1.0 for clear windows. The PDF peaks for thermochromic windows between 0.2 and 0.3 and for clear windows between 0.5 and 0.6. The CDF values for DGP below 0.4, commonly referred to as glare autonomy, are 71 %, 87 %, 89 %, and 70 % for single, double, vacuum, and ventilation glazing, respectively. In contrast, the glare autonomy for clear windows is only around 10–12 %.

5. Discussion

This study first analyzed the effect of substrate glass on the building performance of TC windows, followed by a comparison of TC windows

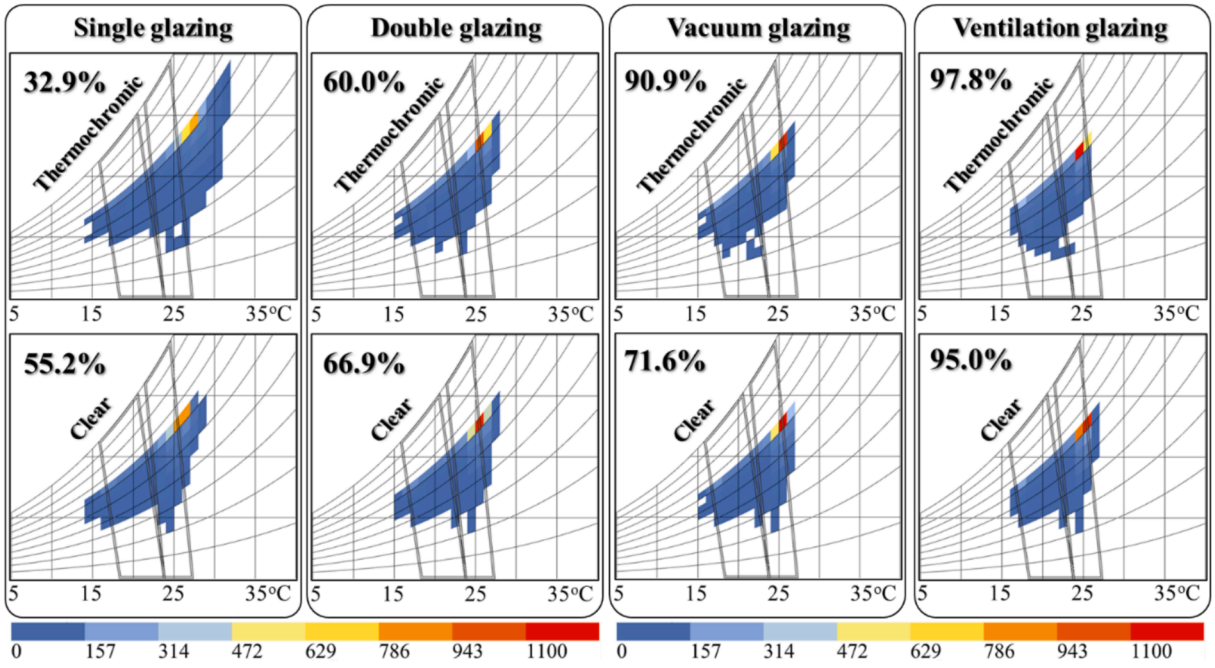

Fig. 13. The indoor thermal comfort condition drawn in the psychrometric chart: (a) Single glazing; (b) Double glazing; (c) Vacuum glazing; (d) Ventilation glazing. The grid inside the polygon represents the acceptable thermal comfort conditions. The color of the grid represents the occupied hours in the present condition.

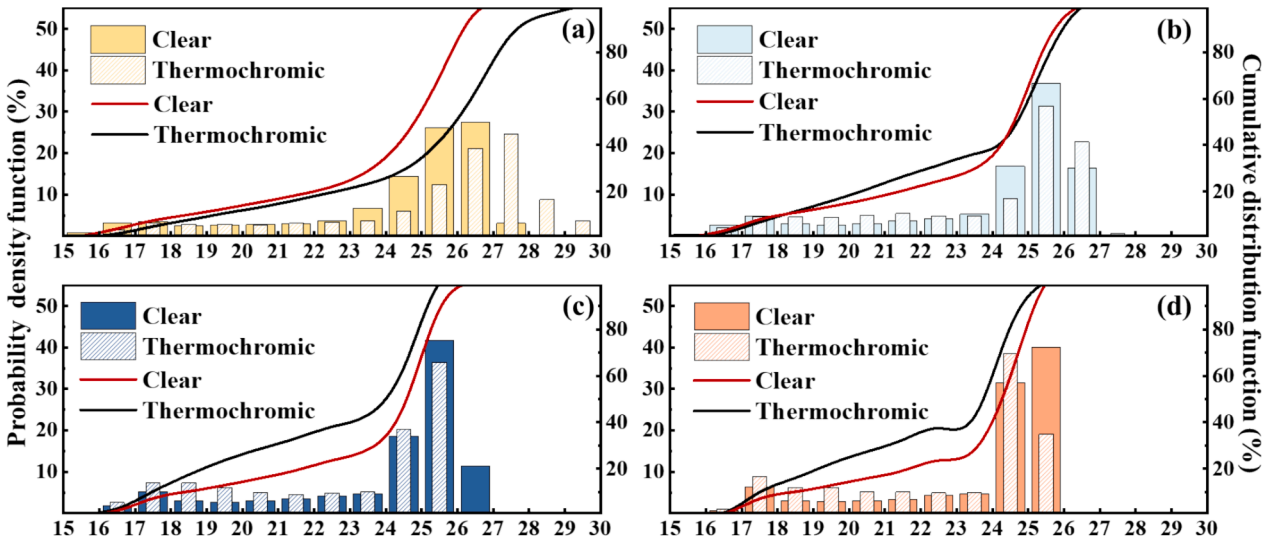

Fig. 14. The distribution of indoor operative temperature: (a) Single glazing; (b) Double glazing; (c) Vacuum glazing; (d) Ventilation glazing.

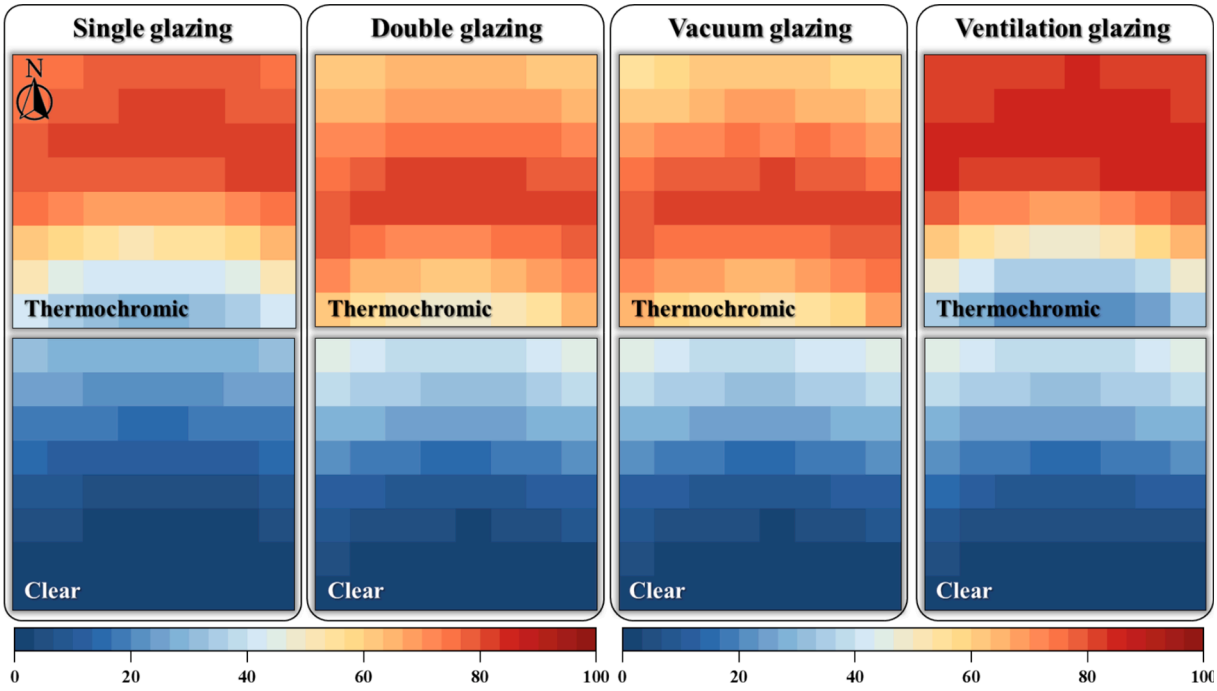

Fig. 15. The distribution of indoor UDI on the work plane (%): (a) Single glazing; (b) Double glazing; (c) Vacuum glazing; (d) Ventilation glazing.

with single, double, vacuum, and ventilation types. The current research mainly emphasizes the impact of structural differences on the performance of TC windows, a critical aspect in the practical application. The analysis results in Section 4 demonstrate that this impact is substantial, but as described in Section 1, previous studies have largely overlooked this aspect. Through quantitative research in this study, some valuable insights can be outlined:

(1) The results presented in Section 4.1 indicate that when the substrate glass has a low absorption rate, such as ultra-clear glass, single or ventilation TC windows fail to undergo the desired state transition. Therefore, the optical properties of the substrate glass must be carefully considered in practical applications. In some cases, simply choosing clear glass may not effectively bring out the energy-saving performance of TC glass. Furthermore, increasing the absorption of near-infrared irradiation shows a more positive impact on building performance than increasing the absorption of visible irradiation. Consequently, it is advisable to select glass with near-infrared selective absorption as the substrate glass of TC materials.

(2) When integrating TC glass, vacuum glazing demonstrates the most significant performance improvements, greater than double glazing, while single glazing shows the least improvement. This indicates that enhancing the thermal insulation performance of windows amplifies the effectiveness of TC glass. Thus, TC glass is highly suitable for combination with windows with thermal insulation strategies, such as transparent insulation materials. The windows with ventilation function can mitigate the negative effects of TC glass due to heat absorption. These findings offer valuable insights for retrofitting buildings with TC technologies and for further development of TC window structures.

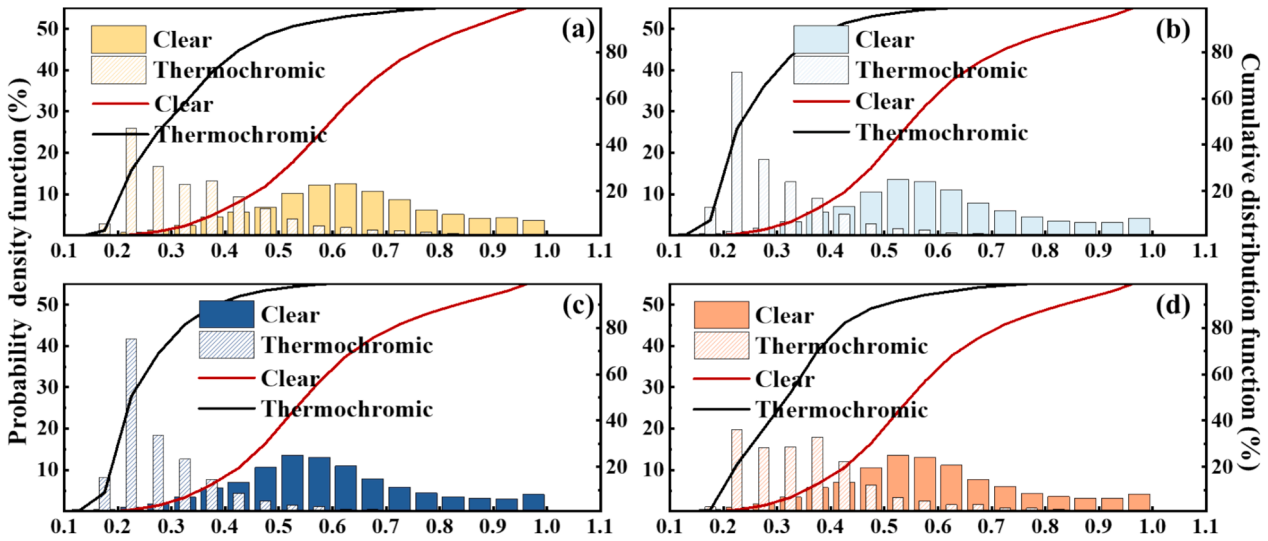

Fig. 16. The distribution of DGP values: (a) Single glazing; (b) Double glazing; (c) Vacuum glazing; (d) Ventilation glazing.

(3) The simulation framework developed in this study can be applied by engineers and architectural designers to evaluate and select window solutions that are tailored to the specific characteristics of any building and its climatic conditions. By integrating window type and building information into the simulation framework, engineers can assess the practicality of TC windows and optimize the properties of TC glass across diverse structural contexts.

By quantitatively analyzing the thermal dynamics of TC windows, this study provides a more comprehensive understanding of how structural factors impact both building energy efficiency and indoor environmental quality. The research results advance the field by exploring how TC materials interact with different window structures. The unique research perspective sets this work apart from previous studies, not only addressing gaps in the literature but also offering practical insights for the design and implementation of TC windows in a variety of building settings.

6. Conclusion

In this study, the energy-saving and human-comfort performance of hydrogel-based TC windows was comprehensively investigated from the structural perspective. Based on the developed simulation framework and the characteristic parameters of hydrogel, an office building in Shenzhen, China was used as the case study for investigating the building performance of single, double, vacuum, and ventilation TC windows, considering the impact of the optical properties of the substrates glass of the hydrogel. The main results are summarized as follows:

(1) The increase in the extinction coefficients of substrate glass increases the time percentage of TC glass in hot state. As the visible extinction coefficients increase, building electricity use initially decreases and then increases, and indoor spatial UDI autonomy initially increases and then decreases. Indoor thermal comfort decreases for single glazing, while other glazing remains almost unaffected. As the near-infrared extinction coefficients increase, building electricity use decreases, and indoor spatial UDI autonomy increases. The change in thermal comfort is consistent with the impact of the visible properties. The global analysis shows that the optimal near-infrared extinction coefficient is 155 to 255 m^{-1}, while the optimal visible extinction coefficient is 55 m^{-1} for double and vacuum glazing and 105 m^{-1} for single and ventilation glazing.

(2) The optimized extinction coefficient is used to explore the performance details of various windows. All types of windows exhibit significant energy-saving effects after integrating TC glass. The reductions and saving ratios in electricity use are: single glazing (249 kWh, 33 %), double glazing (233 kWh, 41 %), vacuum glazing (289 kWh, 51 %), and ventilation glazing (281 kWh, 53 %). For thermal comfort, after installing TC glass, the thermal comfort time for single glazing decreases significantly by 22 %, the change for ventilation and double glazing is not significant, and the thermal comfort time for vacuum glazing increases significantly by nearly 20 %. For visual comfort, after installing TC glass, spatial UDI autonomy of indoor work plane increases by 78 %, 96 %, 100 %, and 72 %, while glare autonomy increases by 60 ~ 80 %.

CRediT authorship contribution statement

Chuyao Wang: Writing – review & editing, Writing – original draft, Software, Methodology, Investigation, Formal analysis, Data curation, Conceptualization. **Sai Liu:** Writing – review & editing, Writing – original draft, Investigation, Data curation. **Xin Li:** Writing – review & editing, Software, Investigation, Data curation. **Qiuyi Shi:** Writing – review & editing, Investigation, Data curation. **Wenqi Wang:** Writing – review & editing, Software, Investigation. **Yang Fu:** Writing – review & editing, Investigation. **Jianheng Chen:** Writing – review & editing, Software, Investigation. **Chi Yan Tso:** Writing – review & editing, Writing – original draft, Supervision, Funding acquisition, Conceptualization.

Declaration of competing interest

The authors declare that they have no known competing financial interests or personal relationships that could have appeared to influence the work reported in this paper.

Acknowledgement

This work was supported by the Hong Kong Research Grant Council via General Research Fund (GRF) account of 11200121.

Appendix A. . Model validation of thermal and daylighting models

As described in Section 3.2, this study employed the EnergyPlus and Radiance software to simulate the thermal and daylighting performance of buildings with TC windows. The hot and cold states of the TC glass were automatically switched using the EMS approach. To validate the reliability of this method, experimental data from Ref [50] was used for model validation. In the referenced study, the authors installed a hydrogel TC window with a transition temperature of 25 °C on the south-facing wall of a test room, which had a 39 % window-to-wall ratio. Indoor temperature and illuminance, as well as meteorological parameters, were continuously measured in Xiamen, China. The geometric parameters of the test room, along with the thermal and optical properties of the building envelope—including the wall and window—from the referenced study were input into the thermal and daylighting models described in Section 3.2. The weather data from the referenced study was input by modifying the weather files to serve as the boundary conditions for model validation. The comparison between the calculated values and the measured results is shown in Fig. A1. It can be observed that the calculated results are in good agreement with the experimental data. To assess simulation accuracy, the mean bias error (MBE) and the coefficient of root mean square error (Cv(RMSE)) were used as evaluation metrics, in alignment with ASHRAE Guideline 14. After performing the calculations based on the relevant equations [60], the Cv(RMSE) and MBE for indoor temperature were found to be 4.2 % and 1.1 %, respectively, while for indoor illuminance, the Cv(RMSE) and MBE were 3.6 % and 0.7 %, respectively. These error analysis results are well below the thresholds specified in ASHRAE Guideline 14, which are 30 % for Cv(RMSE) and 10 % for MBE. This demonstrates that the method used in this study to calculate the thermal and daylighting performance of TC windows is robust and reliable.

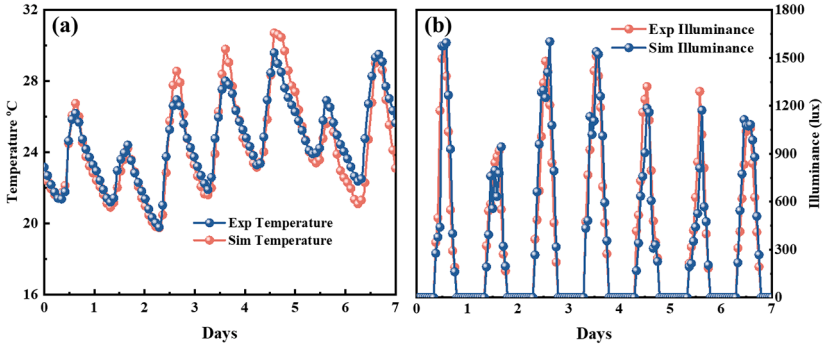

Fig. A1. The comparison between the calculated values and the measured results in Ref [50]. (a) Thermal behavior. (b) Daylighting behavior.

Appendix B. . Model validation of optical model

In this study, the optical model of TC glass in Section 3.2.1 was validated using experimental data from Ref [46]. In the referenced study, the authors measured the optical properties of a three-layer glazing sample consisting of a TC hydrogel membrane laminated between two glass slides at different temperatures. The transition temperature of the TC hydrogel in the referenced study is 28 °C. The transmittance and reflectance of the TC hydrogel membrane at different temperatures, along with the refractive index and extinction coefficient of the glass slides, were input into the optical model used in this study. Subsequently, the overall transmittance and reflectance of the three-layer glazing sample were calculated. A comparison between the calculated values from the present model and the measured results is shown in Fig. B1. It can be observed that the calculated values are in good agreement with the measured results. Particularly for transmittance, which is crucial to building thermal and daylighting performance, the difference between the two is negligible. Therefore, it can be concluded that the net radiation method employed in this study accurately simulates the optical properties of hydrogel-based TC glass.

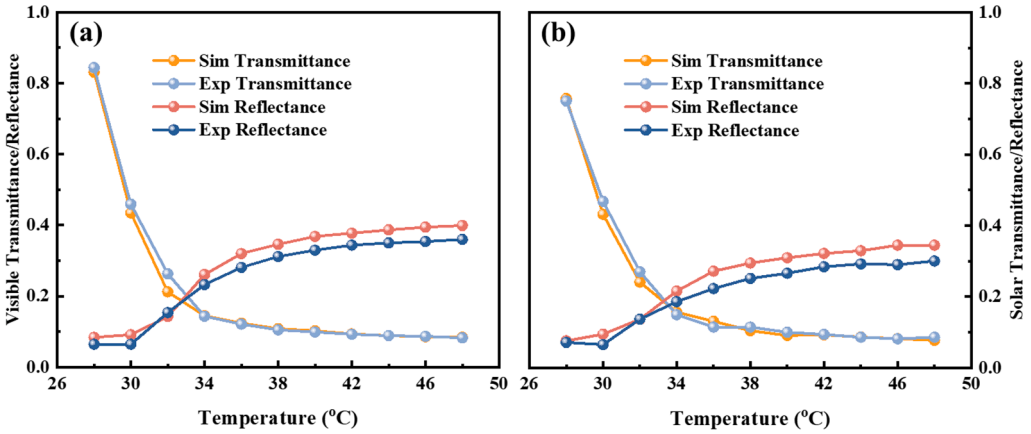

Fig. B1. The comparison between the calculated values and the measured results in Ref [46]. (a) Visible properties. (b) Solar properties.

Data availability

Data will be made available on request.

References

[1] M.N. Mustafa, M.A.A. Mohd Abdah, A. Numan, A. Moreno-Rangel, A. Radwan, Khalid M, A review. Renewable and Sustainable Energy Reviews, Smart window technology and its potential for net-zero buildings, 2023, p. 181.

[2] S.W. Tong, W.P. Goh, X. Huang, C. Jiang, A review of transparent-reflective switchable glass technologies for building facades, Renewable and Sustainable Energy Reviews. 152 (2021).

[3] S. Wu, H. Sun, M. Duan, H. Mao, Y. Wu, H. Zhao, B. Lin, Applications of thermochromic and electrochromic smart windows: Materials to buildings, Cell Reports Physical Science. 4 (5) (2023).

[4] T. Jiang, X. Zhao, X. Yin, R. Yang, G. Tan, Dynamically adaptive window design with thermo-responsive hydrogel for energy efficiency, Applied Energy. 287 (2021).

[5] M. Aburas, V. Soebarto, T. Williamson, R. Liang, H. Ebendorff-Heidepriem, Wu Y, A review. Applied Energy, Thermochromic smart window technologies for building application, 2019, p. 255.

[6] S. Babulanam, T. Eriksson, G. Niklasson, C. Granqvist, Thermochromic VO2 films for energy-efficient windows, Solar Energy Materials. 16 (5) (1987) 347–363.

[7] Z. Zhang, L. Zhang, Y. Zhou, Y. Cui, Z. Chen, Y. Liu, et al., Thermochromic Energy Efficient Windows: Fundamentals, Recent Advances, and Perspectives, Chem Rev. 123 (11) (2023) 7025–7080.

[8] L. Zhang, F. Xia, J. Yao, T. Zhu, H. Xia, G. Yang, et al., Facile synthesis, formation mechanism and thermochromic properties of W-doped VO2(M) nanoparticles for smart window applications, Journal of Materials Chemistry c. 8 (38) (2020) 13396–13404.

[9] H. Guo, Y.G. Wang, H.R. Fu, A. Jain, F.G. Chen, Influence of dopant valence on the thermochromic properties of VO2 nanoparticles, Ceramics International. 47 (15) (2021) 21873–21881.

[10] H. Sun, D. Chen, L. Zhou, W. Mi, D. Wang, L. He, J. Zhao, The synergistic effect of Ta-doping and antireflective TaO layer on the thermochromic VO2 thin films for smart windows, Solar Energy Materials and Solar Cells. 275 (2024).

[11] Y. Zhou, S. Zhao, S. Qi, Y. Liu, N. Chen, L. Wang, et al., VO2 Nanoparticles-Based Thermochromic Smart Windows, ChemistrySelect. 8 (33) (2023).

[12] M. Azmat, S. Shoaib, L.Q. Hajra, H. Jin, J. Li, Enhancing Thermochromic Properties for Thermal Regulation: A Synergistic Study of Er–W-Codoped Vanadium Dioxide (VO2), ACS Applied Energy Materials. 7 (15) (2024) 6746–6756.

[13] S. Liu, C.Y. Tso, Y.W. Du, L.C. Chao, H.H. Lee, T.C. Ho, M.K.H. Leung, Bioinspired thermochromic transparent hydrogel wood with advanced optical regulation abilities and mechanical properties for windows, Applied Energy. 297 (2021).

[14] G. Chen, K. Wang, J. Yang, J. Huang, Z. Chen, J. Zheng, et al., Printable Thermochromic Hydrogel-Based Smart Window for All-Weather Building Temperature Regulation in Diverse Climates, Adv Mater. 35 (20) (2023) e2211716.

[15] S. Liu, Y. Du, R. Zhang, H. He, A. Pan, T.C. Ho, et al., Perovskite Smart Windows: The Light Manipulator in Energy-Efficient Buildings, Adv Mater. 36 (17) (2024) e2306423.

[16] B.A. Rosales, J. Kim, V.M. Wheeler, L.E. Crowe, K.J. Prince, M. Mirzokarimov, et al., Thermochromic Halide Perovskite Windows with Ideal Transition Temperatures, Advanced Energy Materials. 13 (12) (2023).

[17] R. Guo, Y. Shen, Y. Chen, C. Cheng, C. Ye, S. Tang, KCA/Na2SiO3/PNIPAm hydrogel with highly robust and strong solar modulation capability for thermochromic smart window, Chemical Engineering Journal. 486 (2024).

[18] R. Zhang, B. Xiang, Y. Shen, L. Xia, L. Xu, Q. Guan, S. Tang, Energy-efficient smart window based on a thermochromic microgel with ultrahigh visible transparency and infrared transmittance modulation, Journal of Materials Chemistry a. 9 (32) (2021) 17481–17491.

[19] J. Yoon, K.S. Kim, W.K. Hong, Thermochromic Vanadium Dioxide Nanostructures for Smart Windows and Radiative Cooling, Chemistry. 30 (43) (2024) e202400826.

[20] W. Jin, K. Park, J.Y. Cho, S.-H. Bae, M. Siyar, H. Jang, C. Park, Thermochromic properties of ZnO/VO2/ZnO films on soda lime silicate glass deposited by RF magnetron sputtering, Ceramics International. 49 (7) (2023) 10437–10444.

[21] X. Wu, M. Tang, L. Yuan, J. Li, L. Qi, X. Weng, C. Gu, Solvethermal synthesis and thermochromic properties of CaF2@VO2-based core-shell structure composites, Ceramics International. 50 (20) (2024) 37676–37683.

[22] Z. Wang, J. Liang, D. Lei, C. Jiang, Z. Yang, G. Yang, et al., Temperature-adaptive smart windows with passive transmittance and radiative cooling regulation, Applied Energy. 369 (2024).

[23] X. Zhao, J. Sun, J. Ma, T. Liu, Z. Guo, Z. Yang, et al., Combining reversible addition-fragmentation chain transfer polymerization and thiol-ene click reaction for application of core-shell structured VO2@polymer nanoparticles to smart window, Sustainable Materials and Technologies. 32 (2022).

[24] S. Liu, Y. Li, Y. Wang, Y. Du, K.M. Yu, H.L. Yip, et al., Mask-inspired moisture-transmitting and durable thermochromic perovskite smart windows, Nat Commun. 15 (1) (2024) 876.

[25] Z. Liang, X. Liao, J. Yu, Z. Zhou, H. Wang, T. Zhang, et al., Long-Term Stability and Efficiency of VO2 Nanostructure-Based Thermochromic Smart Windows, ACS Applied Nano Materials (2024).

[26] Q. Jiang, M. Chen, Z. Qin, Y. Li, J. Li, H. Zhang, Stable and thermochromic organohydrogels for thermostatically controlled display windows, Chemical Engineering Journal. 489 (2024).

[27] G. Zhu, X. Gang, Y. Zhang, G. Lu, X. Cai, W. Zhang, et al., Thermochromic Smart Windows with Ultra-High Solar Modulation and Ultra-Fast Responsive Speed Based on Solid-Liquid Switchable Hydrogels, Research. 7 (2024).

[28] S. Liu, Y.W. Du, C.Y. Tso, H.H. Lee, R. Cheng, S.P. Feng, K.M. Yu, Organic Hybrid Perovskite (MAPbI3−xClx) for Thermochromic Smart Window with Strong Optical Regulation Ability, Low Transition Temperature, and Narrow Hysteresis Width, Advanced Functional Materials. 31 (26) (2021).

[29] G.R. Araújo, H. Teixeira, M.G. Gomes, A.M. Rodrigues, Multi-objective optimization of thermochromic glazing properties to enhance building energy performance, Solar Energy. 249 (2023) 446–456.

[30] Y. Tao, X. Fang, H. Zhang, G. Zhang, J. Tu, L. Shi, Impacts of thermo-optical properties on the seasonal operation of thermochromic smart window, Energy Conversion and Management. 252 (2022).

[31] M. Arnesano, G. Pandarese, M. Martarelli, F. Naspi, K.L. Gurunatha, C. Sol, et al., Optimization of the thermochromic glazing design for curtain wall buildings based on experimental measurements and dynamic simulation, Solar Energy. 216 (2021) 14–25.

[32] K. Khaled, U. Berardi, Z. Liao, Energy modelling and saving potential of polymeric solar-responsive thermochromic window films, Solar Energy. 244 (2022) 84–103.

[33] S. Wu, H. Sun, J. Song, S. Liu, S. Shi, C. Tso, B. Lin, Comprehensive analysis on building performance enhancement based on selective split-band modulated adaptive thermochromic windows, Applied Energy. 372 (2024).

[34] R. Liang, Y. Sun, M. Aburas, R. Wilson, Y. Wu, An exploration of the combined effects of NIR and VIS spectrally selective thermochromic materials on building performance, Energy and Buildings. 201 (2019) 149–162.

[35] L. Hu, H. Zhu, K. Lu, C. Wang, L. Liu, L. Ma, Theoretical investigation of VO2 smart window with large-scale dynamic infrared emittance adjustment for adaptive thermal management, Solar Energy. 277 (2024).

[36] C. Haratoka, R.A. Yalcin, H. Erturk, Design of thermo-chromic glazing windows considering energy consumption and visual comfort for cellular offices, Solar Energy. 241 (2022) 637–649.

[37] J. Wang, G. Li, D. Zhao, Multi-objective optimization of an anti-reflection AlN/VO2/AlN thermochromic window for building energy saving, Energy. 288 (2024).

[38] C. Haratoka, R.A. Yalcin, H. Erturk, Examination of energy and visual comfort performance of thermo-chromic coatings for cellular offices, Energy. 267 (2023).

[39] M. Salamati, P. Mathur, G. Kamyabjou, K. Taghizade, Daylight performance analysis of TiO2@W-VO2 thermochromic smart glazing in office buildings, Building and Environment. 186 (2020).

[40] M. Aburas, H. Ebendorff-Heidepriem, L. Lei, M. Li, J. Zhao, T. Williamson, et al., Smart windows – Transmittance tuned thermochromic coatings for dynamic control of building performance, Energy and Buildings. 235 (2021).

[41] Y. He, S. Liu, C.Y. Tso, A novel solar-based human-centered framework to evaluate comfort-energy performance of thermochromic smart windows with advanced optical regulation, Energy and Buildings. 278 (2023).

[42] Y. Sun, X. Liu, Y. Ming, X. Liu, D. Mahon, R. Wilson, et al., Energy and daylight performance of a smart window: Window integrated with thermotropic parallel slat-transparent insulation material, Applied Energy. 293 (2021).

[43] Y. Ming, Y. Sun, X. Liu, X. Liu, Y. Wu, Thermal performance of an advanced smart fenestration systems for low-energy buildings, Applied Thermal Engineering. 244 (2024).

[44] S. Wang, Y. Zhou, T. Jiang, R. Yang, G. Tan, Y. Long, Thermochromic smart windows with highly regulated radiative cooling and solar transmission, Nano Energy. 89 (2021).

[45] Y. Ding, C. Zhong, F. Yang, Z. Kang, B. Li, Y. Duan, et al., Low energy consumption thermochromic smart windows with flexibly regulated photothermal gain and radiation cooling, Applied Energy. 348 (2023).

[46] X. Liu, Y. Wu, Numerical evaluation of an optically switchable photovoltaic glazing system for passive daylighting control and energy-efficient building design, Building and Environment. 219 (2022).

[47] S. Xu, C. Li, W. He, W. Chu, Z. Hu, B. Lu, Experimental study of bifacial photovoltaic wall system incorporating thermochromic material, Sustainable Cities and Society. 106 (2024).

[48] H. Teixeira, M. Glória Gomes, A. Moret Rodrigues, D. Aelenei, Assessment of the visual, thermal and energy performance of static vs thermochromic double-glazing under different European climates, Building and Environment. 217 (2022).

[49] N. Es-sakali, S. Idrissi Kaitouni, I. Ait Laasri, M. Oualid Mghazli, M. Cherkaoui, J. Pfafferott, Static and dynamic glazing integration for enhanced building efficiency and indoor comfort with thermochromic and electrochromic windows, Thermal Science and Engineering Progress. 52 (2024).

[50] F. Shi, Y. You, X. Yang, X. Hong, Annual evaluation of the visual-thermal comfort and energy performance of thermotropic glazing in a reference office room of China, Building and Environment. 254 (2024).

[51] R. Liang, M. Kent, R. Wilson, Y. Wu, The effect of thermochromic windows on visual performance and sustained attention, Energy and Buildings. 236 (2021).

[52] Y. Shen, P. Xue, T. Luo, Y. Zhang, C.Y. Tso, N. Zhang, et al., Regional applicability of thermochromic windows based on dynamic radiation spectrum, Renewable Energy. 196 (2022) 15–27.

[53] Michaux G, Greffet R, Salagnac P, Ridoret JBJAE. Modelling of an airflow window and numerical investigation of its thermal performances by comparison to conventional double and triple-glazed windows. 2019;242(PT.1-1284):27-45.

[54] J. Huang, Q. Wang, X. Chen, S. Xu, H. Yang, Experimental investigation and annual overall performance comparison of different photovoltaic vacuum glazings, Sustainable Cities and Society. 75 (2021).

[55] S. Liu, Y. Li, Y. Wang, K.M. Yu, B. Huang, C.Y. Tso, Near-Infrared-Activated Thermochromic Perovskite Smart Windows, Adv Sci (weinh). 9 (14) (2022) e2106090.

[56] C. Wang, H. Yang, J. Ji, Investigation on overall energy performance of a novel multi-functional PV/T window, Applied Energy. 352 (2023).
[57] Y. Zhou, X. Dong, Y. Mi, F. Fan, Q. Xu, H. Zhao, et al., Hydrogel smart windows, Journal of Materials Chemistry a. 8 (20) (2020) 10007–10025.
[58] J. Peng, D.C. Curcija, A. Thanachareonkit, E.S. Lee, H. Goudey, S.E. Selkowitz, Study on the overall energy performance of a novel c-Si based semitransparent solar photovoltaic window, Applied Energy. 242 (2019) 854–872.
[59] International Glass Data Base. Available online: https://windows.lbl.gov/igdb-downloads. [Accessed 2 July 2024].
[60] M. Wang, J. Peng, N. Li, H. Yang, C. Wang, X. Li, T. Lu, Comparison of energy performance between PV double skin facades and PV insulating glass units, Applied Energy. 194 (2017) 148–160.
[61] C. Zhang, J. Ji, C. Wang, W. Ke, H. Xie, B. Yu, Experimental and numerical studies on the thermal and electrical performance of a CdTe ventilated window integrated with vacuum glazing, Energy. 244 (2022).
[62] C. Wang, H. Yang, J. Ji, Design, fabrication, and performance assessment of a novel PV/T double skin facade, Building and Environment (2024).
[63] Fujian Super Tech Advanced Material Co., Ltd. Available online: http://www.vip-vig.com. [Accessed 2 June 2024].
[64] F. Chen, G. Lu, H. Yuan, R. Li, J. Nie, Y. Zhao, et al., Mechanism and regulation of LCST behavior in poly(hydroxypropyl acrylate)-based temperature-sensitive hydrogels, Journal of Materials Chemistry a. 10 (35) (2022) 18235–18247.
[65] Iso, 15099, Thermal performance of windows, doors and shading devices —, Detailed Calculations. (2003).
[66] M.M. Uddin, C. Wang, C. Zhang, J. Ji, Investigating the energy-saving performance of a CdTe-based semi-transparent photovoltaic combined hybrid vacuum glazing window system, Energy. 253 (2022).
[67] G. Gennaro, E. Catto Lucchino, F. Goia, F. Favoino, Modelling double skin façades (DSFs) in whole-building energy simulation tools: Validation and inter-software comparison of naturally ventilated single-story DSFs, Building and Environment. 231 (2023).
[68] M. Wang, J. Peng, N. Li, L. Lu, T. Ma, H. Yang, Assessment of energy performance of semi-transparent PV insulating glass units using a validated simulation model, Energy. 112 (2016) 538–548.
[69] Y. Bian, Y. Chen, Y. Sun, Y. Ma, D. Yu, T. Leng, Simulation of daylight availability, visual comfort and view clarity for a novel window system with switchable blinds in classrooms, Building and Environment. 235 (2023).
[70] M. Talaei, H. Sangin, Multi-objective optimization of energy and daylight performance for school envelopes in desert, semi-arid, and mediterranean climates of Iran, Building and Environment. 255 (2024).
[71] F. Salata, I. Golasi, W. Verrusio, V.E. de Lieto, M. Cacciafesta, V.A. de Lieto, On the necessities to analyse the thermohygrometric perception in aged people. A review about indoor thermal comfort, health and energetic aspects and a perspective for future studies, Sustainable Cities and Society. 41 (2018) 469–480.
[72] ISO 7730, Ergonomics of the thermal environment — Analytical determination and interpretation of thermal comfort using calculation of the PMV and PPD indices and local thermal comfort criteria. 2005.
[73] C. Wang, M.M. Uddin, J. Ji, B. Yu, J. Wang, The performance analysis of a double-skin ventilated window integrated with CdTe cells in typical climate regions, Energy and Buildings. 241 (2021).
[74] Commercial Reference Buildings. Available online: https://www.energy.gov/eere/buildings/commercial-reference-buildings. [Accessed 2 June 2024].
[75] Y. Tan, J. Peng, Z. Luo, Y. Luo, T. Ma, J. Ji, et al., Multi-function partitioned design method for photovoltaic curtain wall integrated with vacuum glazing towards zero-energy buildings, Renewable Energy. 218 (2023).
[76] C. Wang, H. Yang, J. Ji, Performance analysis of a PV/T shading device for enhancing energy saving and human comfort, Applied Energy. 376 (2024).
[77] ASHRAE Standard 55: Thermal Environmental Conditions for Human Occupancy. 2023.
[78] GB 50736-2012. Design code for heating ventilation and air conditioning of civil buildings. 2012.
[79] GB 19576-2019. Minimum allowable values of energy efficiency and energy efficiency grades for unitary air conditioners. 2019.
[80] GB 50033-2013. Standard for daylighting design of buildings. 2013.